Identification of quantitative trait loci (QTL) and meta-QTL analysis for kernel size-related traits in wheat (Triticum aestivum L.)

Jingfu Ma
Gansu Agricultural University
Yuan Liu
Gansu Agricultural University
Peipei Zhang
Gansu Agricultural University
Tao Chen
Gansu Agricultural University
Tian Tian
Gansu Agricultural University
Peng Wang
Gansu Agricultural University
Zhuo Che
Plant Seed Master Station of Gansu Province
Fahimeh Shahinnia
Institute for Crop Science and Plant Breeding
Delong Yang (yangdl@gsau.edu.cn)
Gansu Agricultural University

Research Article

Keywords: Wheat, Kernel size, MQTL analysis, Gene expression, Candidate gene

Posted Date: August 12th, 2022

DOI: https://doi.org/10.21203/rs.3.rs-1931220/v1

Abstract

Background

Kernel size-related traits, as critical determinants of wheat kernel weight and yield potential, are complex quantitative traits controlled by polygenes. Genome-wide identification of important and stable quantitative trait loci (QTL) and functional genes for these traits can advance molecular genetic improvement of wheat kernel yield.

Results

In this study, Thirty-two QTLs for kernel size-related traits, including kernel length (KL), kernel width (KW), kernel diameter ratio (KDR) and kernel thickness (KT), were discovered using a series of recombinant inbred lines (RILs) which explained 3.06–14.2% of the phenotypic variation. Of these, eleven QTLs were confirmed as stable QTLs in multiple environments. The 1103 original QTLs from 34 previous studies and the present study were employed for the MQTL analysis, in which 346 of the 1103 original QTLs were refined to 58 MQTLs. Compared to the original QTLs, the average confidence intervals of the target MQTLs decreased 3.26-fold, but the average genetic contribution rates to explain phenotypic variation increased 1.72-fold. Through comprehensive analysis of wheat publicly available transcriptome data, a total of 70 putative candidate genes for kernel size development were ultimately identified within the MQTL regions.

Conclusions

kernel size-related traits predominantly regulated by genetic factors and can be detected in different water conditions. Potential candidate genes expressed in spike and grain were identified through meta-QTL and in-silico expression analysis. The identification of stable QTLs and candidate genes for kernel size-related traits provides a novel insight to understand the genetic basis of kernel size-related traits in wheat.

Background

Wheat (*Triticum aestivum* L.) is one of the most important cereal crops worldwide, providing nearly 40% of the calories for the world population [1]. It is estimated that wheat yield needs to be increased by 70% to meet the food demand associated with the growth of the world population [2]. In this context, improving wheat yield is critical to ensuring food security in the future. Wheat yield is mainly influenced by thousand kernel weight (TKW), number of kernels per spike (KNS), and reproductive pollen number (RTN) [3, 4]. Of these, TKW has been selected as an important target trait in wheat breeding programs due to its high heritability [5]. Kernel size-related traits, as one of the critical factors in kernel weight formation, were mainly composed of kernel length (KL), kernel width (KW), kernel diameter ratio (KDR), and kernel thickness (KT) [6]. Larger kernels have a positive influence on the growth performance of wheat seedlings

and contribute greatly to yield improvement [4, 7–8]. Deciphering the genetic basis and finding functional genes for kernel size are critical for enhancement of grain yield and quality traits in wheat.

Traits related to grain size in wheat have attracted considerable attention in crop breeding. These are complex quantitative traits controlled by polygenes [9–11] and are strongly influenced by both genotypic and environmental factors [12]. In the last two decades, a large number of QTLs underlying wheat kernel size-related traits have been successfully identified by traditional bi-parental linkage mapping [7, 9–11, 13–17] and genome-wide association studies (GWAS) [18–23]. However, due to the redundancy of functional genes in three sub-genomes A, B, and D of wheat and the highly repetitive nature of this genome, identifying stable and robust QTLs for kernel size-related and yield traits remains challenging [24, 25]. Therefore, identification and validation of reliable QTLs for controlling these traits remain crucial in wheat breeding.

Previous study reported that QTLs for grain size were generally mapped in large confidence intervals with small effects and are significantly influenced by genetic background and environment, which limits the usefulness of these QTLs in wheat breeding programs [26]. Meta-QTL analysis is a robust method for genetic analysis of complex traits and an effective approach to integrate QTLs from different pathways to obtain stable genetic regions controlling a quantitative trait [27]. Compared to QTLs identified in a single study, MQTLs have the advantage of having a smaller QTL confidence interval and being stable across multiple experimental runs. Meta-QTL analysis may also overcome the limitations of identifying candidate genes in a genome as complex as wheat.

MQTL analysis have been successfully applied in various crops, including maize [28–31], rice [26, 32–33], and soybean [34]. MQTL analysis in wheat have also been effectively used to establish the consensus map of QTLs for many agronomic traits. Previous study integrated QTLs for yield and yield-related traits from published articles and identified 12 significant MQTLs on chromosome 1A, 1B, 2A, 2D, 3B, 4A, 4B, 4D, and 5A including two important underlying genes such as *Rht* and *Vrn* [35]. Tyagi et al. (2015) performed a meta-analysis of QTLs associated with kernel morphological traits and mapped 17 MQTLs on 7 chromosomes in wheat [36]. In previous study, a total of 2230 QTLs for yield and yield-related traits were used for meta-QTL analysis and identified 145 MQTLs, of which 85 were verified by GWAS using different natural populations, within 76 MQTL core intervals, 237 candidate genes involved in photoperiod response, kernel development, multiple plant growth regulatory pathways, carbon and nitrogen metabolism, and ear and flower organ development were identified through searching for sequence homology and expression analysis [37]. Meanwhile, Liu et al. (2020) performed a meta-analysis with 381 QTL related to yield and identified 86 MQTL and 210 candidate genes in wheat [38]. In addition to yield-related traits, MQTL analysis were also used to discover consistent QTLs and identification of candidate genes for various quantitative traits such as leaf rust [39], drought and heat tolerance [40–42], salt tolerance [43], and disease resistance [44–46].

In the present study, the inclusive composite interval mapping (ICIM) method was used to identify the QTL controlling kernel size-related traits across seven environments. We performed a meta-analysis by

combining the QTLs detected in our study with the 1071 QTLs from previous studies. Our main objectives were to: (1) identify stable QTL for traits related to kernel size in seven environments; (2) discover and map MQTLs from numerous reported QTL and current studies; (3) identify candidate genes related to kernel size associated with MQTL intervals.

Results

Phenotypic and correlation analyses

In the field trials conducted in seven environments (E1-E7), the parental line Q9086 had a significantly longer and wider kernel compared to Longjian19 (Table S1). In KT, the parental line Longjian19 had an advantage over Q9086. In the RILs population, all traits varied widely and had an approximately normal distribution with obvious transgressive segregation (Fig. 1). The coefficients of variation for KL, KW, KDR, and KT ranged from 3.47–5.71%, 2.47–6.27%, 3.24–8.57%, and 3.88–5.45%, respectively. ANOVA of the four kernel size-related traits revealed significant differences ($P < 0.01$) among environments, genotype and genotye × environment interaction. Among the kernel size-related traits, KL ($h^2 = 0.89$) and KDR ($h^2 = 0.70$) were highly heritable, followed by KW ($h^2 = 0.67$) and KT ($h^2 = 0.61$) (Table S2).

Significant correlations were found among KL, KW, KDR, and KT (Fig. 2). KL showed a positive correlation with KW ($r = 0.45$, $P < 0.01$) and KDR ($r = 0.71$, $P < 0.01$), whereas there was a negative correlation with KT ($r = -0.03$, $P < 0.05$). KW showed a positive correlation with KT ($r = 0.41$, $P < 0.01$) and KDR ($r = -0.30$, $P < 0.05$). In addition, a negative correlation was observed between KT and KDR ($r = -0.42$, $P < 0.01$).

QTLs controlling kernel size-related traits

QTL mapping detected 32 QTLs for kernel size-related traits with the PVE ranging from 3.06–14.2% in different environments (Table S3, Fig. 3). These loci were mapped on 17 of the 21 chromosomes, except for chromosomes 2B, 4B, 5A, and 5D. Eleven stable QTLs, namely *QKL.acs-1A*, *QKW.acs-1A*, *QKDR.acs-2A*, *QKL.acs-2D*, *QKW.acs-3A*, *QKDR.acs-4A*, *QKDR.acs-5B.2*, *QKL.acs-6A*, *QKL.acs-6B*, *QKW.acs-7B.1*, and *QKW.acs-7B.2*, were detected in more than three environments, with PVE ranging from 3.07–9.85%.

Ten QTLs associated with KL were identified on chromosomes 1A, 1B, 2D, 3D, 4A, 6A, 6B, 7A, 7B, and 7D, with PVE ranging from 3.40–8.26% (Table S3, Fig. 3). Of these, four stable QTLs were identified for KL on chromosomes 1A, 2D, 6A, and 6B, including *QKL.acs-1A* identified in E3, E4 and E5, *QKL.acs-2D* identified in E3, E4 and E7, *QKL.acs-6A* identified in E3, E5 and E7, and *QKL.acs-6B* identified in E1, E2, E3, E6 and E7, respectively. Notably, *QKL.acs-6B*, with 4.07–8.26% of the PVE, was detected in five environments (E1, E2, E3, E6 and E7). Except for the QTL *QKL.acs-6B*, the additive effect of other three stable QTLs contributed to decreasing of KL.

Among the seven QTLs associated with KW on six chromosomes (1A, 2D, 3A, 4A, 4D, and 7B), with PVEs ranged from 3.35–9.85% (Table S3, Fig. 3), four stable QTLs, *QKW.acs-1A* identified in E4, E6 and E7,

QKW.acs-3A identified in E2, E3 and E6, *QKW.acs-7B.1* identified in E4, E5 and E6, and *QKW.acs-7B.2* identified in E1, E5 and E6, which were mapped on chromosomes 1A, 3A, and 7B, respectively. *QKW.acs-1A* and *QKW.acs-7B.1* had a negative additive effect on KW, while *QKW.acs-3A* and *QKW.acs-7B.2* showed a positive additive effect for increasing KW. The QTLs *QKW.acs-7B.1* and *QKW.acs-7B.2* were detected on the same chromosomes with opposite additive effects.

Nine QTLs were identified for KDR with individual PVEs ranging from 3.06–14.2% distributed on eight chromosomes (1A, 1D, 2A, 2D, 3B, 3D, 4A, and 5B) (Table S3, Fig. 3). Three stable QTLs, *QKDR.acs-2A* identified in E1, E5 and E7, *QKDR.acs-4A* identified in E2, E3, E6 and E7, and *QKDR.acs-5B.2* identified in E1, E3 and E5, were also detected in at least three environments with a range of PVE between 3.06–6.9%. A major QTL *QKDR.acs-2D* was identified and contributed to explaining 14.2% of phenotypic variance. In addition, a stable QTL *QKDR.acs-4A* was detected in four environments (E2, E3, E6 and E7) and accounted for 3.06–6.9% of the PVE.

On the chromosomes 2A, 3B, 4D, 6A, 6B, and 6D, six QTLs associated with KT were identified, each accounting for 4.6–10% of PVE (Table S3, Fig. 3). They were all detected in less than two environments. Among those, QTL *QKT.acs-3B.1* owned the highest PVE of 10%.

QTLs identified under different water environments

In our study, we detected 19 QTL for kernel size-related traits under WW environments and 14 QTLs under DS environments, the last of which mapped on chromosomes 1A, 1B, 1D, 2D, 3B, 3D, 4A, 5B, 6A, 6B, and 7D, with an average PVE of 5.83% (Table S3, Fig. 3). Two stable QTLs, *QKL.acs-2D* and *QKW.acs-1A*, were identified under DS conditions. Under WW environments, nine QTLs for kernel size-related traits were located on chromosomes 1A, 2A, 3D, 4A, 4D, 6D, 7A, and 7B with an average PVE of 6.30%. Importantly, nine stable QTLs, including *QKL.acs-1A*, *QKDR.acs-2A*, *QKW.acs-3A*, *QKDR.acs-4A*, *QKDR.acs-5B.2*, *QKL.acs-6A*, *QKL.acs-6B*, *QKW.acs-7B.1*, and *QKW.acs-7B.2*, were identified under both WW and DS environments.

Initial QTLs collection for wheat kernel size-related traits

A total of 34 QTL studies published between 2007 and 2020 for KL, KW, KDR, and KT were used for MQTL analysis (Table S4). By integrating 1071 initial QTLs from 34 studies and 32 QTLs discovered in this study, a total of 1103 initial QTLs for kernel size-related traits were used for MQTL analysis (Fig. 4a). The distribution of QTLs across homologous groups, sub-genomes, and individual chromosomes was not uniform. For example, the number of QTLs ranged from 101 on homologous group VII to 241 on group II, and from 15 on chromosome 4D to 117 on chromosome 2D (Fig. 4b). Of the 1103 initial QTLs, 399, 433 and 271 QTLs were distributed among sub-genomes A, B and D, respectively (Fig. 4d). The confidence interval ranged from 0.14 cM to 190 cM, with an average of 14.52 cM (Fig. 4c). The proportion of phenotypic variance explained by individual QTL ranged from 1.00–86.31%, with an average of 9.98% (Fig. 4c).

MQTL analysis for wheat kernel size-related traits

A total of 346 initial QTLs were located on the consensus map, while the remaining QTLs were eliminated due to the lack of common markers with the consensus map (Fig. 5). After meta-analysis, 58 MQTLs were detected on chromosomes 1B, 1D, 2A, 3D, 4A, 5B, 5D, 6B, 7A, 7B, and 7D (Table S5). Each chromosome harboured 2 (3D) to 7 MQTLs (1B, 4A, 7B) (Fig. 6a), and the projected initial QTLs on the chromosomes varied from 20 (5D) to 80 (5B) (Fig. 6b). Most of the MQTL regions were co-localized for more than two kernel size-related features (Fig. 5). The number of individual QTL per MQTL ranged from 1 (MQTL37 and MQTL38) to 18 (MQTL18) (Table S5). MQTL intervals ranged from 0.21 cM (MQTL33) to 72.64 cM (MQTL46) with an average of 4.46 cM, representing a reduction of 3.26-fold compared to the initial QTLs (14.54 cM) (Table S5, Fig. 6c). The PVE ranged from 5% (MQTL7) to 56% (MQTL35) with an average PVE of 17.12%, which was increased 1.72-fold (Table S5, Fig. 6d). Based on the comparison of the flanking marker sequences, the MQTLs had unique physical positions in the reference sequence of the Chinese Spring wheat genome. The physical interval of these 58 MQTLs ranged from 1.54 Kb to 580.66 Mb (Table S5). Particularly, 12 MQTLs with a physical interval < 20 Mb were selected as target MQTLs.

Candidate genes mining and expression analysis

We identified 1864 potential candidate genes in 12 MQTL intervals, with the lowest (1) and highest (487) number of potential candidate genes in the MQTL50 and MQTL15 intervals, respectively. The potential candidate genes in the interval of the 12 MQTLs were screened and annotated based on the wheat reference genome of the Chinese Spring as the version of IWGSC RefSeq v1.1 (Table S6).

The GO terms associated with biological processes belonged to metabolic and cellular (229 and 210 candidate genes, respectively) pathways (Fig. 7). GO terms associated with molecular function were related to binding and catalytic activity (380 and 260 candidate genes, respectively). Regarding the cellular component, candidate genes were mainly related to the cell and cell part with 130 and 128 candidate genes, respectively. KEGG analysis for candidate genes revealed that the ubiquitin-mediated proteolysis and plant hormone signalling are the two most important pathways involved in the metabolic process (Fig. 8).

The potential candidate genes were then subjected to *in silico* expression analysis using publicly available various RNAseq data. Only 70 candidate genes belonging to 9 MQTLs (except MQTL50, MQTL51, and MQTL55) were differentially expressed in spike and grain (Table 1, Fig. 9). These genes are involved in various metabolic pathways, such as carbon fixation in photosynthetic organisms (4 candidate genes), carbon metabolism (6 candidate genes), mRNA surveillance pathway (4 candidate genes), RNA transport (4 candidate genes), and biosynthesis of secondary metabolites (18 candidate genes).

Table 1
Identification of 70 candidate genes located in the nine core MQTL intervals

MQTL	Gene ID	Gene Position	Description	Orthology
MQTL9	TraesCS1D02G004900	2218794–2230403	Paired amphipathic helix protein Sin3	NA
	TraesCS1D02G005200	2468742–2472416	Glycosyltransferase-like KOBITO 1	Os01g13200
	TraesCS1D02G007800	3961444–3964988	Ankyrin repeat family protein	Os01g01960
	TraesCS1D02G007900	3968895–3969443	MICOS complex subunit Mic25	Os05g01300
MQTL15	TraesCS2A02G083000	38218064–38220520	Elongation factor 1-alpha	Os03g08010
	TraesCS2A02G083300	38304986–38306906	Elongation factor 1-alpha	Os03g08010
	TraesCS2A02G086400	39704402–39709256	AAA + ATPase domain	*OsRpt3*; *OSRPT2B*
	TraesCS2A02G087000	40541031–40547241	Adenosine/AMP deaminase domain	Os07g49270
	TraesCS2A02G088300	41652179–41655428	NmrA-like domain	Os12g16410
	TraesCS2A02G089300	42470945–42476145	Heat shock transcription factor	*OsHsfA2b*; *OsHSF5*
	TraesCS2A02G090000	43133651–43137076	AAA + ATPase domain	*OSRPT2B*
	TraesCS2A02G092200	45085317–45085622	Wound-induced protein WI12	Os03g18770
	TraesCS2A02G075800	33696041–33701785	DNA binding	Os04g19684
	TraesCS2A02G076700LC	38490262–38490831	Pol polyprotein	Os04g20220
	TraesCS2A02G076900	34517930–34520662	ER membrane protein complex subunit 8/9-like protein	Os04g20230
	TraesCS2A02G079500	36047811–36053052	Oxoglutarate dehydrogenase (succinyl-transferring) activity	Os07g49520

MQTL	Gene ID	Gene Position	Description	Orthology
	TraesCS2A02G080000	36138685–36141909	LPS-induced tumor necrosis factor alpha factor	Os02g31100
	TraesCS2A02G082100	37084649–37088462	Peroxidase activity	*OsAPX1*; *OsAPXa*
	TraesCS2A02G075900	33712839–33714236	Leucine-rich repeat 2	*OsFbox194*
MQTL19	TraesCS3D02G024500	8285414–8287617	Glyceraldehyde-3-phosphate dehydrogenase	Os01g02930
	TraesCS3D02G024700	8336528–8341354	Cytochrome P450	*OsCYP709C5*
	TraesCS3D02G026400	8971472–8975036	Fructose-bisphosphate aldolase class-I	Os11g07020
	TraesCS3D02G031900	11747403–11752024	WD40 repeat	*OsAIP1*
	TraesCS3D02G032000	11755792–11762962	Ubiquitin-conjugating enzyme E2	*OsUBC34*
MQTL22	TraesCS4A02G472900LC	605125402–605129635	Putative S-adenosyl-L-methionine-dependent methyltransferase	Os01g62800
	TraesCS4A02G473000LC	605128287–605128517	S-adenosyl-L-methionine-dependent methyltransferases superfamily protein	NA
	TraesCS4A02G315500	605656378–605659792	Chaperonin Cpn60	Os12g17910
	TraesCS4A02G310700	603377077–603380232	Zinc finger C2H2-type	Os09g39660
MQTL26	TraesCS4A02G442900	710742945–710744427	Peroxisomal biogenesis factor 11	Os06g03660
	TraesCS4A02G445300	713352055–713352438	Ozone-responsive stress-related protein	Os06g02420
MQTL40	TraesCS6B02G772700LC	701661949–701662457	ATP-dependent 6-phosphofructokinase 1	NA
	TraesCS6B02G432600	701871210–701874404	Thiolase	*OsI57*
	TraesCS6B02G432700	701886743–701890627	Ribosomal protein L13	Os08g06474

MQTL	Gene ID	Gene Position	Description	Orthology
	TraesCS6B02G432900	701977549–701982043	Aldo/keto reductase family	Os02g57240
	TraesCS6B02G433800	702562152–702565516	DHHC palmitoyltransferase	*OsPAT15*
	TraesCS6B02G434700	703153107–703155841	OTU-like cysteine protease	Os02g57410
	TraesCS6B02G436400	704038894–704042474	Serine-threonine protein phosphatase N-terminal domain	*OsPP41*
	TraesCS6B02G439300	704879300–704881854	PBS lyase HEAT-like repeat	Os12g43100
	TraesCS6B02G439400	704882414–704885861	Target SNARE coiled-coil homology domain	Os02g57510
	TraesCS6B02G783000LC	704944589–704949129	ATP binding	NA
	TraesCS6B02G439800	705158924–705162882	RING/U-box superfamily protein	Os11g18947
	TraesCS6B02G440000	705282693–705285851	B3 DNA binding domain	Os03g42230
	TraesCS6B02G440200	705377945–705384852	Metabolic process	Os06g19960
	TraesCS6B02G440500	705497185–705500263	Fibrillarin	Os02g57590
MQTL47	TraesCS7B02G002900	1203205–1208405	COP1-interacting-like protein	*DEP2*; *EP2*; *SRS1*
	TraesCS7B02G005700	3142605–3150879	THIF-type NAD/FAD binding fold	Os02g30310
	TraesCS7B02G005800LC	2014362–2018322	NAC domain	Os01g18070
	TraesCS7B02G003000	1254814–1262214	COP1-interacting-like protein	*DEP2*; *EP2*; *SRS1*
	TraesCS7B02G003200	1277537–1282562	PB1 domain	Os07g25680
MQTL49	TraesCS7B02G366700	630552409–630552871	Ubiquitin domain	Os06g46770
	TraesCS7B02G619400LC	632490144–632492343	GTPase activity	NA

MQTL	Gene ID	Gene Position	Description	Orthology
	TraesCS7B02G377800	642274924–642277145	Ribosomal protein S8	Os02g15610
	TraesCS7B02G636000LC	644027912–644028247	Myosin-like protein XIG	NA
	TraesCS7B02G623100LC	634562940–634564127	F-box protein At5g41490	NA
	TraesCS7B02G370800	636625334–636627607	Ribosomal protein S13	Os03g58050
	TraesCS7B02G371900	637769054–637774747	RNA recognition motif domain	Os06g45910
	TraesCS7B02G372500	638129949–638134271	SANT/Myb domain	Os06g01670
	TraesCS7B02G372700	638509625–638515329	Conserved oligomeric Golgi complex subunit 7	Os06g45830
	TraesCS7B02G373000	638882526–638885183	Peptidase M41	*OsFtsH2*
MQTL55	TraesCS7D02G148900	96756606–96777587	Chromatin-remodeling factor CHD3	*CHR702*
	TraesCS7D02G149000	97615140–97617186	SWEET sugar transporter	*OsSWEET15*
	TraesCS7D02G149300	98292586–98293620	Rtf2 RING-finger	Os06g08490
	TraesCS7D02G149500	98408253–98411417	DNA-directed RNA polymerase subunit beta	*DPL2*
	TraesCS7D02G149800	98637892–98644179	Ubiquitin carboxyl-terminal hydrolase	Os06g08530
	TraesCS7D02G150300	99617003–99618245	Thioredoxin-like fold	Os07g09310
	TraesCS7D02G150900	100280693–100281019	Proteolipid membrane potential modulator	*OsRCI2-8*
	TraesCS7D02G152400	101084476–101087850	Glutathione peroxidase	*OsGPX4*
	TraesCS7D02G152800	101395597–101400935	Serine-type carboxypeptidase activity	*OsSCP1*
	TraesCS7D02G153200	101580722–101585530	ATP-dependent DNA helicase	Os06g08740

MQTL	Gene ID	Gene Position	Description	Orthology
	TraesCS7D02G154500	102537242–102539785	RNA-binding (RRM/RBD/RNP motifs) family protein	Os10g39510

Discussions

Grain yield is influenced by the combination of kernel weight and number per spike [14, 47]. TKW is not only one of the key components of grain yield, but also is commonly used as a standard factor for determining flour quality and marketing in wheat. Kernel size and shape, including KL, KW, and KT, are strongly and positively correlated with TKW [48–50]. A bigger kernel has a positive effect on wheat kernel weight and yield, improving flour quality and commercial value [38, 51]. Kernel size-related traits influence wheat yield by regulating TKW, and both are associated with high heritability [16, 52–57].

We observed significant and positive correlations between KL, KW, and KDR (r = 0.45 and r = 0.71, respectively), KW and KT (r = 0.41, P < 0.01). Meanwhile, a negative and significant correlation was also observed between KT and KDR (r = -0.42, P < 0.01) (Fig. 2), which is consistent with previous studies [13, 48, 58–59]. It is known that KL reached its maximum value 15 days after anthesis, while KW and KT reached their maximum value two weeks later [60, 61]. KL showed the highest heritability (0.89) in this study, followed by KDR (0.70), KW (0.67), and KT (0.61) (Table S2), which is consistent with previous studies [7, 60–62]. Therefore, increasing KL and KW through genetic improvement can have a positive effect on grain weight and yield of wheat.

Traits related to kernel size are known to influence TKW strongly. Many QTLs and genes for kernel size have been identified on 21 chromosomes in wheat [16, 59, 62–65, 67–68]. In this study, 32 QTLs for KL, KW, KDR, and KT were found on 17 chromosomes, suggesting that genetic factors play an important role in kernel size-related traits (Table S3, Fig. 3). *QKW.acs-1A*, a stable QTL identified in E4, E6, and E7, is in the *Xcfa2219-Xgwm99* interval on chromosome 1A and was detected only under DS environments. Li et al. (2012) identified a major QTL with a PVE of 40.79% that shares the same flanking marker *Xgwm99* with *QKW.acs-1A* [69]. In addition, the stable QTLs *QKL.acs-1A* and *QKW.acs-1A* share the same flanking marker *Xwmc99* with the QTLs *QGw.ccsu-1A.3* reported by Mir et al. (2012) [70]. *Xgwm99* can be used for marker-assisted selection in wheat breeding programs. *QKL.acs-2D*, located in the interval of *Xgwm157-Xwmc41*, shared a common flanking marker (*Xwmc41*) with *QTKW.ncl-2D.2* [52]. *QKL.acs-2D*, located in the *Xgwm157-Xwmc41* interval on chromosome 2D, strongly overlapped with the different environmental QTLs for KDR (*QKDR.acs-2D*) and KW (*QKW.acs-2D*). In addition, *QKL.acs-6B* was identified in E1, E2, E3, E6, and E7, with a PVE ranging from 4.07–8.26%, suggesting that kernel size-related traits are closely linked and represent one of the crucial elements in the regulation of kernel weight.

As a result of QTL mapping studies in different environments, numerous QTLs for kernel size-related traits have been identified. MQTL analysis is a useful tool to effectively integrate QTLs reported in

different studies and to remove the barriers such as genetic background, population type, and environmental variations in QTL mapping [27, 71]. We conducted MQTL analysis using a total of 1071 QTLs controlling kernel size-related traits detected in 34 independent previous studies and 32 QTLs identified in the present study (Table S4, Fig. 4). These original QTLs were unevenly distributed across 21 chromosomes, and most of them were located on sub-genomes A and B, consistent with previous studies [35, 37]. In this study, 346 original QTLs were refined into 58 MQTLs and distributed on chromosomes 1B, 1D, 2A, 3D, 4A, 5B, 5D, 6B, 7A, 7B, and 7D (Table S5, Fig. 5). Each chromosome harbor 2 MQTLs (3D) to 7 MQTLs (1B, 4A, 7B), and the projected original QTL numbers on the chromosomes varied from 20 (5D) to 80 (5B). The distribution of MQTLs and original QTLs on different chromosomes is inconsistent due to the different number of original QTLs contained in MQTLs [37]. In the present study, the average 95% confidence interval of MQTL (4.46 cM) was 3.26-fold smaller than that of the original QTLs (14.54 cM), and the average PVE of MQTLs (17.12%) was 1.72-fold larger than that of the original QTLs (9.95%) (Fig. 6c, 6d), while the average confidence interval of identified MQTLs for yield-related traits was 2.9-fold lower than that of the original QTLs [37]. Most of the MQTLs in the present study controlled more than one trait, likely indicating either tight linkage of genes or the presence of pleiotropic genes for controlling kernel size-related traits [37, 41, 46, 71].

Candidate genes related to important agronomic traits have been identified by MQTL analysis [37–38, 41, 72–73]. Nadolska-Orczyk et al (2017) classified genes related to controlling kernel yield into five categories, including transcription factors, growth regulator signalling, carbohydrate metabolism, cell division and proliferation, and flowering regulators [74]. Understanding the genetic and physiological pathways involving in grain development is of great help for investigating of traits related to kernel size. In our study, we detected 1864 candidate genes in 12 MQTL intervals with a physical interval less than 20 Mb using the wheat genome reference sequence of Chinese Spring. Among 1864 candidate genes, 70 candidate genes were expressed mainly in the spike and grain at different developmental stages (Table 1, Fig. 9), consistent with previously reported by Yang et al. (2021) [37]. In recent years, analysis of homology relationships between wheat and rice facilitated cloning of several yield-related genes such as *TaFlo-A1* [75], *TaCKX6-D1* [76], and *TaTGW6-A1* [77]. Here, 17 out of 70 candidate genes homologous to rice genes were found within MQTL intervals, such as *TraesCS3D02G024700*, which is homologous to *OsCYP709C5* [78], a gene involved in the regulation of cytochrome P450, discovered in the MQTL19 interval. Guo et al. (2021) also showed that constitutive overexpression of *TaCYP78A5* significantly increased seed size and weight [79]. The ubiquitin-proteasome pathway has been associated with seed size development in both wheat and rice, and the corresponding genes *e.g., TaGW2-6A/6B* [80, 81] and *OsUBC* [82] have been cloned in wheat and rice, respectively. According to previous study, carbohydrate metabolism is an important factor affecting yield and yield-related traits [74]. In this study, *TraesCS7D02G149000* (MQTL55), its homologous gene *OsSWEET15* [83] and *TaSWEETs* [84, 85] were identified as important genes involving in sucrose transport pathway in rice. In addition, floral regulators are also an important regulator in the regulation of yield and yield-related traits [74]. The *TraesCS7D02G149500* (MQTL55) was identified as an orthologous gene of *DPL1/2*, involving in pollen hybrid incompatibility in rice [86]. In our study, the orthologous genes of *DEP2*, *EP2*, and *SRS1* were found

in MQTL47 (*TraesCS7B02G002900*, *TraesCS7B02G003000*), which was shown to be related to kernel size and yield [87, 88]. In addition, the remaining 53 candidate genes were involved in various signalling pathways, such as zinc finger protein [89], transcription factors [17], and glycosyltransferase [90], are also involved in the regulation of yield and yield-related traits.

Conclusions

In this study, we found that kernel size-related traits in wheat predominantly regulated by genetic factors with a moderate and high heritability. Most of stable QTLs were detected under both well-watered and drought-stressed conditions. Potential candidate genes expressed in spike and grain were identified through meta-QTL and *in-silico* expression analysis. The markers closely linked to stable QTL had great potential in marker-assisted breeding program and the identification of potential candidate genes advanced the understanding of the genetic basis regulating the processes of kernel size in wheat.

Methods

Plant materials and field trials

A set of wheat hexaploid RILs population was used in this study. The RILs population consists of 120 lines derived from the cross between two winter wheat cultivars, Longjian19 and Q9086 [91]. The male parent, Longjian19, released by the Gansu Academy of Agricultural Sciences, Lanzhou, Gansu, is an elite drought-tolerant variety widely grown in rainfed areas (300–500 mm annual rainfall) in northwest China. The female parent Q9086, released by Northwest Agriculture&Forestry University, Yangling, Shanxi, is a high-yielding variety developed by Northwest Agriculture and Forestry University, China. It is suitable for cultivation under conditions with adequate water and high fertility, but is sensitive to water and fertilizer conditions, especially at the grain-filling stage. The two parents differ significantly from several physiological and agronomical traits, especially under rainfed environments [91–93].

Field trials were conducted at Yuzhong farm station, Gansu, China (35°48'N, 104°18'E, altitude 1860 m) during the growing seasons in 2015–2016 under drought-stressed (DS, designated E1) and well-watered conditions (WW, designated E2), while in 2016–2017 only under drought-stressed conditions (designated E3). Field trials were also conducted at Tongwei farm station, Gansu, China (35°11'N, 105°19'E, altitude 1750 m) during the 2017–2018, 2018–2019, and 2019–2020 growing seasons. Planting in 2017–2018 was conducted under drought-stressed (designated E4) and well-watered conditions (designated E5), while the 2018–2019 and 2019–2020 cropping seasons were conducted under drought-stressed conditions only (designated E6 and E7, respectively). The two cropping sites are characterized by a typical dry inland environmental condition in Northwest China, where the annual average temperature is about 7.0°C, the annual rainfall is less than 400 mm with approximately 60% falling from July to September, but the annual evapotranspiration capacity is more than 1500 mm. The DS treatments were equivalent to rainfed condition in each growing season, whereas the WW treatments were irrigated with the water supply of 75 mm at the spike emergence (Zadoks 55) and grain filling (Zadoks 71) stages,

respectively. Here, the decimal codes for growth stages of wheat described by Zadoks et al (1974) [94]. In this case, the rainfall of the DS plots in each field environment was 164.3 mm (E1) to 296.5 mm (E7) (Fig. S1). All progenies and parents were sown in late September and harvested in early July of the following year. A randomized complete block design (RCBD) was conducted with three replications for each line and parent. Each plot consisted of six 1 m rows, 0.2 m spacing, with a sowing rate of 60 seeds per row. Field management followed local wheat cultivation practices.

After harvesting, two hundred seeds for each line were used to measure kernel length (KL), kernel width (KW), and kernel diameter ratio (KDR) with the SC-G wheat grain appearance quality image analysis system (Hangzhou WSeen Detection Technology Co., Ltd, Hangzhou, China) with three biological replicates, while kernel thickness (KT) was measured with vernier caliper. All data were recorded in millimetres (mm). The average values of the traits were used for QTL analysis.

Statistical analysis

Statistical analysis and analysis of variance (ANOVA) were performed using SPSS 22.0 (IBM Corporation, Armonk, NY, United States). Following the method described by Toker et al. (2004) [95], the broad-sense heritability (h^2) was estimated across environments using the formula:

$$h^2 = \sigma_g^2 / \left(\sigma_g^2 + \sigma_{ge}^2 / r + \sigma_e^2 / re\right)$$

where σ_g^2, σ_{ge}^2 and σ_e^2 estimate genotype, genotype×environment interaction and residual error variances, respectively, and *e* and *r* are the numbers of environments and replicates per environment, respectively. The correlation among KL, KW, KDR, and KT in the RILs population was also assessed.

Construction of linkage map and QTL analysis

For QTL mapping, a genetic map consisted of 524 SSR markers, described in a previous study was used [96]. These markers were distributed among 21 linkage groups and covered a total genetic distance of 2266.72 cM with an average distance of 4.33 cM between adjacent markers.

The inclusive composite interval mapping (ICIM) method was performed using the QTL software IciMapping V4.1 to determine the positions and effects of QTLs [97]. QTL with LOD value ≥ 2.5, as determined by 1000 permutation tests at $P \leq 0.05$, were declared for the presence of significant QTL. QTL were named based on the International Rules for Genetic Nomenclature (http://wheat.pw.usda.gov/ggpages/wgc/98/intro.htm). QTLs detected in at least three of seven environments were considered as stable QTL. QTLs for a trait identified with common flanking markers or overlapping confidence intervals were treated as one QTL, with the confidence interval reassigned by overlapping genetic positions. The phenotypic variance explained (PVE) by QTLs was estimated according to previous studied [16, 98–99].

Initial QTL collections used for MQTL analysis

A total of 1071 QTLs for KL, KW, KDR, and KT traits derived from 36 bi-parental populations were retrieved from 34 published studies from 2007 to 2020 (Table S4). The size of the mapping populations varied from 99 to 547 lines of different types, including 3 double haploid (DH), 7 F_2, and 26 RILs populations evaluated in different years and locations. The population information, including target traits, population parents, population types, and number of markers used in genetic map was listed in Table S4.

QTLs localization on reference map

A high-density map containing 7352 markers, including SSR, DArT, SNP, and other types of markers, was used as a reference map in this study [73]. The total length of the reference map is 4994.0 cM with an average distance of 0.68 cM. The original QTL data and associated individual genetic maps from previous studies, as well as the reference map, were used as input files to create a consensus map (Fig. S2) and perform MQTL analysis with BioMercator V4.2.3 [100].

The position, chromosome groups, proportion of phenotypic variance explained (PVE or R^2), and logarithm of odds ratio (LOD score) were recorded for each of the QTL in the 36 studies. To calculate 95% confidence intervals (CI) for QTLs, the formula CI = 530/(N×R^2) for BC and F_2 lines, CI = 287/(N×R^2) for DH lines, and CI = 163/(N×R^2) for RILs lines was applied, where N is the population size and R^2 is the proportion of phenotypic variance explained of the QTL [101]. For QTLs without well-defined LOD scores and R^2, these criteria were arbitrarily set at 3 and 10%, respectively. All collected QTLs with appropriate information were projected onto the reference map using BioMercator V4.2.3 [100]. The approach proposed by Goffinet and Gerber [27] was used when the number of QTLs per chromosome was 10 or less, while the two-step algorithm of Veyrieras [102] was used when the number of QTLs per chromosome was higher than 10. The Akaike Information Criterion (AIC) statistics were used to determine the best model for defining the number of MQTLs or "true" QTLs that best represent the original QTLs. The algorithms and statistical procedures implemented in this software are well described in previous studies [100, 102–103].

Identification of candidate genes

To identify candidate genes, initially the marker or its related primer sequences on both sides of the MQTL confidence intervals were manually searched using URGI Wheat (https://wheat-urgi.versailles.inra.fr), GrainGenes (https://wheat.pw.usda.gov/GG3/), DArT (https://www.diversityarrays.com), and the Illumina company (https://www.illumina.com) databases. The obtained sequences were then aligned to IWGSC RefSeq v1.1 (https://wheat-urgi.versailles.inra.fr/) to find the physical location of each marker. Putative candidate genes for this MQTL with a physical interval of less than 20 Mb were identified and their associated functions were compared to choose the best possible candidates. The candidate genes were also investigated using Gene Ontology (GO) and Kyoto Encyclopedia of Genes and Genomes (KEGG) enrichment analyses using Omicshare online tools (https://www.omicshare.com/).

In-silico expression analysis of candidate genes

The transcriptomic data of several wheat tissues deposited in the Expression Visualization and Integration Platform (expVIP, https://www.wheat-expression.com/) were downloaded to study the *in-silico* tissue expression of candidate genes [104]. This included 18 tissues throughout the wheat growth period [105]. The expression levels of candidate genes were assessed by transcripts per million (TPM) and visualized using the heatmap of TBtools software (https://github.com/CJChen/TBtools/releases).

Abbreviations

AIC, Akaike Information Criterion; ANOVA, analysis of variance; BC, back cross; CG, candidate genes; CI, confidence interval; cM, centimorgan; DH, double haploid; DS, drought-stressed; GO, Gene Ontology; GWAS, genome-wide association study; h^2, broad-sense heritability; ICIM, inclusive composite interval mapping; KDR, kernel diameter ratio; KEGG, Kyoto Encyclopedia of Genes and Genomes; KL, kernel length; KNS, number of kernel per spike; KT, kernel thickness; KW, kernel width; LOD, logarithm of odds ratio; MQTL, Meta-QTL; PVE, phenotypic variation explained; QTL, quantitative trait loci; RCBD, randomized complete block design; RIL, recombinant inbred lines; RTN, reproductive pollen number; SNP, single nucleotide polymorphic; SSR, simple sequence repeat; TKW, thousand kernel weight; TPM, transcripts per million; WW, well-watered.

Declarations

Ethics approval and consent to participate

We declare that the experiments comply with the ethical standards and legislations in China, and all wheat varieties were collected in accordance with national guidelines.

Consent for publication

Not applicable

Availability of data and materials

All data generated or analyzed during this study are included in this published article and its supplementary information files. The datasets used and/or analyzed during the current study are available from the corresponding author on reasonable request. The original QTL mapping datasets presented in this study can be found in online repositories.

Competing interests

The authors declare that they have no competing interests.

Funding

This work was financially supported by the Research Program Sponsored by State Key Laboratory of Aridland Crop Science, China (GHSJ 2020-Z4), the Key Research and Development Program of Gansu Province, China (21YF5NA089), Industrial Support Plan of Colleges and Universities in Gansu Province (2022CYZC-44), and the National Natural Science Foundation of China (31760385).

Authors' contributions

JM and DY conceived of the study. JM, PZ, TT, PW performed phenotypic evaluations and data analysis. YL, PZ, TC, ZC and FS prepared the figures, provided scientific comments and reviewed the content. JM wrote the first draft of the manuscript. DY and FS revised and edited the manuscript. All authors have read and agreed to the published version of the manuscript.

Acknowledgements

We are grateful to Prof. Guohong Zhang (Institute of Dryland Agriculture, Gansu Academy of Agricultural Science, Lanzhou, Gansu, China) for providing the wheat materials.

References

1. Comastri A, Janni M, Simmonds J, Uauy C, Pignone D, Nguyen HT, Marmiroli N. Heat in wheat: exploit reverse genetic techniques to discover new alleles within the triticum durum shsp26 family. Frontiers in Plant Science. 2018; 9: 1–16. https://doi.org/10.3389/fpls.2018.01337.
2. Langridge P. Wheat genomics and the ambitious targets for future wheat production. Genome. 2013; 56(10): 545–547. https://doi.org/10.1139/gen-2013-0149.
3. Hawkesford MJ, Araus JL, Park R, Calderini D, Miralles D, Shen T, Zhang J, Parry AJ. Prospects of doubling global wheat yields. Food and Energy Security. 2013; 2(1): 34–48. https://doi.org/10.1002/fes3.15.
4. Kesavan M, Song JT, Seo HS. Seed size: A priority trait in cereal crops. Physiologia Plantarum. 2013; 147(2): 113–120. https://doi.org/10.1111/j.1399-3054.2012.01664.x.
5. Sehgal D, Mondal S, Guzman C, Garcia Barrios G, Franco C, Singh R, Dreisigacker S. Validation of Candidate Gene-Based Markers and Identification of Novel Loci for Thousand-Grain Weight in Spring Bread Wheat. Frontiers in Plant Science. 2019; 10: 1189-1202. https://doi.org/10.3389/fpls.2019.01189.
6. Dholakia BB, Ammiraju SS, Singh H, Lagu MD, Röder MS, Rao VS, Dhaliwal HS, Ranjekar PK, Gupta VS. Molecular marker analysis of kernel size and shape in bread wheat. Plant Breeding. 2003;122(5): 392–395. https://doi.org/10.1046/j.1439-0523.2003.00896.x.
7. Gegas VC, Nazari A, Griffiths S, Simmonds J, Fish L, Orford S, Sayers L, Doonan JH, Snape JW. A genetic framework for grain size and shape variation in wheat. Plant Cell. 2010; 22(4): 1046–1056. https://doi.org/10.1105/tpc.110.074153.

8. Wang S, Li S, Liu Q, Wu K, Zhang J, Wang S, Wang Y, Chen X, Zhang Y, Gao C, Wang F, Huang H, Fu X. The *OsSPL16* - *GW7* regulatory module determines grain shape and simultaneously improves rice yield and grain quality. Nature Genetics. 2015; 47:949-954. https://doi.org/10.1038/ng.3352.
9. Williams K, Sorrells ME. Three-dimensional seed size and shape QTL in hexaploid wheat (*Triticum aestivum* L.) populations. Crop Science. 2014; 54(1): 98–110. https://doi.org/10.2135/cropsci2012.10.0609.
10. Kumari S, Jaiswal V, Mishra VK, Paliwal R, Balyan HS, Gupta PK. QTL mapping for some grain traits in bread wheat (*Triticum aestivum* L.). Physiology and Molecular Biology of Plants. 2018; 24(5): 909–920. https://doi.org/10.1007/s12298-018-0552-1.
11. Hu J, Wang X, Zhang G, Jiang P, Chen W, Hao Y, Ma X, Xu S, Jia J, Kong L, Wang H. QTL mapping for yield-related traits in wheat based on four RIL populations. Theoretical and Applied Genetics. 2020; 133(3): 917–933. https://doi.org/10.1007/s00122-019-03515-w.
12. Cao S, Xu D, Hanif M, Xia X, He ZH. Genetic architecture underpinning yield component traits in wheat. Theoretical and Applied Genetics. 2020; 133(6): 1811–1823. https://doi.org/10.1007/s00122-020-03562-8.
13. Sun XY, Wu K, Zhao Y, Kong FM, Han GZ, Jiang HM, Huang XJ, Li RJ, Wang HG, Li SS. QTL analysis of kernel shape and weight using recombinant inbred lines in wheat. Euphytica. 2009; 165(3): 615–624. https://doi.org/10.1007/s10681-008-9794-2.
14. Tsilo TJ, Hareland GA, Simsek S, Chao S, Anderson JA. Genome mapping of kernel characteristics in hard red spring wheat breeding lines. Theoretical and Applied Genetics. 2010; 121(4): 717–730. https://doi.org/10.1007/s00122-010-1343-4.
15. Prashant R, Kadoo N, Desale C, Kore P, Dhaliwal HS, Chhuneja P, Gupta V. Kernel morphometric traits in hexaploid wheat (*Triticum aestivum* L.) are modulated by intricate QTL × QTL and genotype × environment interactions. Journal of Cereal Science. 2012; 56(2): 432–439. https://doi.org/10.1016/j.jcs.2012.05.010.
16. Kumar A, Mantovani EE, Seetan R, Soltani A, Echeverry-Solarte M, Jain S, Simsek S, Doehlert D, Alamri MS, Elias EM, Kianian SF, Mergoum M. Dissection of Genetic Factors underlying Wheat Kernel Shape and Size in an Elite × Nonadapted Cross using a High Density SNP Linkage Map. The Plant Genome. 2016; 9(1): 1–22. https://doi.org/10.3835/plantgenome2015.09.0081.
17. Brinton J, Simmonds J, Uauy C. Ubiquitin-related genes are differentially expressed in isogenic lines contrasting for pericarp cell size and grain weight in hexaploid wheat. BMC Plant Biology. 2018; 18(1): 1–17. https://doi.org/10.1186/s12870-018-1241-5.
18. Yan X, Zhao L, Ren Y, Dong Z, Cui D, Chen F. Genome-wide association study revealed that the *TaGW8* gene was associated with kernel size in Chinese bread wheat. Scientific Reports. 2019; 9(1): 2072–2083. https://doi.org/10.1038/s41598-019-38570-2.
19. Muqaddasi QH, Brassac J, Ebmeyer E, Kollers S, Korzun V, Argillier O, Stiewe G, Plieske J, Ganal MW, Röder MS. Prospects of GWAS and predictive breeding for European winter wheat's grain protein

content, grain starch content, and grain hardness. Scientific Reports. 2020; 10(1): 12541–12558. https://doi.org/10.1038/s41598-020-69381-5.

20. Gahlaut V, Jaiswal V, Balyan HS, Joshi AK, Gupta PK. Multi-Locus GWAS for Grain Weight-Related Traits Under Rain-Fed Conditions in Common Wheat (*Triticum aestivum* L.). Frontiers in Plant Science. 2021; 12: 1-13. https://doi.org/10.3389/fpls.2021.758631.
21. Gao L, Meng C, Yi T, Xu K, Cao H, Zhang S, Yang X, Zhao Y. Genome-wide association study reveals the genetic basis of yield- and quality-related traits in wheat. BMC Plant Biology. 2021; 21(1): 1–11. https://doi.org/10.1186/s12870-021-02925-7.
22. Malik P, Kumar J, Sharma S, Meher PK, Balyan HS, Gupta PK, Sharma S. GWAS for main effects and epistatic interactions for grain morphology traits in wheat. Physiology and Molecular Biology of Plants. 2022; 28(3): 651–668. https://doi.org/10.1007/s12298-022-01164-w.
23. Tong J, Zhao C, Sun M, Fu L, Song J, Liu D, Zhang Y, Zheng J, Pu Z, Liu L, Rasheed A, Li M, Xia X, He Z, Hao Y. High Resolution Genome Wide Association Studies Reveal Rich Genetic Architectures of Grain Zinc and Iron in Common Wheat (*Triticum aestivum* L.). Frontiers in Plant Science. 2022; 13: 758631-758644. https://doi.org/10.3389/fpls.2022.840614.
24. Simmonds J, Scott P, Leverington-Waite M, Turner AS, Brinton J, Korzun V, Snape J, Uauy C. Identification and independent validation of a stable yield and thousand grain weight QTL on chromosome 6A of hexaploid wheat (*Triticum aestivum* L.). BMC Plant Biology. 2014; 14(1): 191–204. https://doi.org/10.1186/s12870-014-0191-9.
25. Guan P, Shen X, Mu Q, Wang Y, Wang X, Chen Y, Zhao Y, Chen X, Zhao A, Mao W, Guo Y, Xin M, Hu Z, Yao Y, Ni Z, Sun Q, Peng H. Dissection and validation of a QTL cluster linked to Rht-B1 locus controlling grain weight in common wheat (*Triticum aestivum* L.) using near-isogenic lines. Theoretical and Applied Genetics. 2020; 133(9): 2639–2653. https://doi.org/10.1007/s00122-020-03622-z.
26. Khahani B, Tavakol E, Shariati V, Fornara F. Genome wide screening and comparative genome analysis for Meta-QTLs, ortho-MQTLs and candidate genes controlling yield and yield-related traits in rice. BMC Genomics. 2020; 21: 294–318. https://doi.org/10.1186/s12864-020-6702-1.
27. Goffinet B, Gerber S. Quantitative trait loci: A meta-analysis. Genetics. 2000; 155(1): 463–473. https://doi.org/10.1093/genetics/155.1.463.
28. Coque M, Martin A, Veyrieras JB, Hirel B, Gallais A. Genetic variation for N-remobilization and postsilking N-uptake in a set of maize recombinant inbred lines. 3. QTL detection and coincidences. Theoretical and Applied Genetics. 2008; 117(5): 729–747. https://doi.org/10.1007/s00122-008-0815-2.
29. Truntzler M, Barrière Y, Sawkins MC, Lespinasse D, Betran J, Charcosset A, Moreau L. Meta-analysis of QTL involved in silage quality of maize and comparison with the position of candidate genes. Theoretical and Applied Genetics. 2010; 121(8): 1465–1482. https://doi.org/10.1007/s00122-010-1402-x.

30. Chen L, An Y, Li YX, Li C, Shi Y, Song Y, Zhang D, Wang T, Li Y. Candidate loci for yield-related traits in maize revealed by a combination of metaQTL analysis and regional association mapping. Frontiers in Plant Science. 2017; 8: 2190–2203. https://doi.org/10.3389/fpls.2017.02190.
31. Guo J, Chen L, Li Y, Shi Y, Song Y, Zhang D, Li Y, Wang T, Yang D, Li C. Meta-QTL analysis and identification of candidate genes related to root traits in maize. Euphytica. 2018; 214: 2283-2286. https://doi.org/10.1007/s10681-018-2283-3.
32. Ballini E, More JB, Droc G, Price A, Courtois B, Notteghem JL, Tharreau D. A genome-wide meta-analysis of rice blast resistance genes and quantitative trait loci provides new insights into partial and complete resistance. Molecular Plant-Microbe Interactions. 2008; 21(7): 859–868. https://doi.org/10.1094/MPMI-21-7-0859.
33. Islam MS, Ontoy J, Subudhi PK. Meta-analysis of quantitative trait loci associated with seedling-stage salt tolerance in rice (*Oryza Sativa* L.). Plants. 2019; 8(2): 4–13. https://doi.org/10.3390/plants8020033.
34. Sun YN, Pan JB, Shi XL, Du XY, Wu Q, Qi ZM, Jiang HW, Xin DW, Liu CY, Hu GH, Chen QS. Multi-environment mapping and meta-analysis of 100-seed weight in soybean. Molecular Biology Reports. 2012; 39(10): 9435–9443. https://doi.org/10.1007/s11033-012-1808-4.
35. Zhang LY, Liu DC, Guo XL, Yang WL, Sun JZ, Wang DW, Zhang A. Genomic distribution of quantitative trait loci for yield and yield-related traits in common wheat. Journal of Integrative Plant Biology. 2010; 52: 996–1007. https://doi.org/10.1111/j.1744-7909.2010.00967.x.
36. Tyagi S, Mir RR, Balyan HS. Interval mapping and meta-QTL analysis of grain traits in common wheat (*Triticum aestivum* L.). Euphytica. 2015; 201(3): 367–380. https://doi.org/10.1007/s10681-014-1217-y.
37. Yang Y, Amo A, Wei D, Chai Y, Zheng J, Qiao P, Cui C, Lu S, Chen L, Hu YG. Large-scale integration of meta-QTL and genome-wide association study discovers the genomic regions and candidate genes for yield and yield-related traits in bread wheat. Theoretical and Applied Genetics. 2021; 134: 3083–3109. https://doi.org/10.1007/s00122-021-03881-4.
38. Liu H, Mullan D, Zhang C, Zhao S, Li X, Zhang A, Lu Z, Wang Y, Yan G. Major genomic regions responsible for wheat yield and its components as revealed by meta-QTL and genotype–phenotype association analyses. Planta. 2020; 252(4), 65–77. https://doi.org/10.1007/s00425-020-03466-3.
39. Soriano JM, Royo C. Dissecting the genetic architecture of leaf rust resistance in wheat by QTL meta-analysis. Phytopathology. 2015; 105(12): 1585–1593. https://doi.org/10.1094/PHYTO-05-15-0130-R.
40. Acuña-Galindo MA, Mason RE, Subramanian NK, Hays DB. Meta-analysis of wheat QTL regions associated with adaptation to drought and heat stress. Crop Science. 2015; 55(2): 477–492. https://doi.org/10.2135/cropsci2013.11.0793.
41. Kumar A, Saripalli G, Jan I, Kumar K, Sharma PK, Balyan HS, Gupta PK. Meta-QTL analysis and identification of candidate genes for drought tolerance in bread wheat (*Triticum aestivum* L.).

Physiology and Molecular Biology of Plants. 2020; 26(8): 1713–1725. https://doi.org/10.1007/s12298-020-00847-6.

42. Soriano JM, Colasuonno P, Marcotuli I, Gadaleta A. Meta-QTL analysis and identification of candidate genes for quality, abiotic and biotic stress in durum wheat. Scientific Reports. 2021; 11: 11877–11892. https://doi.org/10.1038/s41598-021-91446-2.
43. Pal N, Saini DK, Kumar S. Meta-QTLs, ortho-MQTLs and candidate genes for the traits contributing to salinity stress tolerance in common wheat (*Triticum aestivum* L.). Physiology and Molecular Biology of Plants. 2021; 27: 2767–2786. https://doi.org/10.1007/s12298-021-01112-0.
44. Liu Y, Salsman E, Wang R, Galagedara N, Zhang Q, Fiedler JD, Liu Z, Xu S, Faris JD, Li X. Meta-QTL analysis of tan spot resistance in wheat. Theoretical and Applied Genetics. 2020; 133(8): 2363–2375. https://doi.org/10.1007/s00122-020-03604-1.
45. Amo A, Soriano JM. Unravelling consensus genomic regions conferring leaf rust resistance in wheat via meta-QTL analysis. The Plant Genome. 2021; 15(1): 1–21. https://doi.org/10.1002/tpg2.20185.
46. Jan I, Saripalli G, Kumar K, Kumar A, Singh R, Batra R, Sharma PK, Balyan HS, Gupta PK. Meta-QTLs and candidate genes for stripe rust resistance in wheat. Scientific Reports. 2021; 11: 1–13. https://doi.org/10.1038/s41598-021-02049-w.
47. Neuweiler JE, Maurer HP, Würschum T. Long-term trends and genetic architecture of seed characteristics, grain yield and correlated agronomic traits in triticale (× *Triticosecale Wittmack*). Plant Breeding. 2020; 139(4): 717–729. https://doi.org/10.1111/pbr.12821.
48. Xiao Y, He S, Yan J, Zhang Y, Zhang Y, Wu Y, Xia X, Tian J, Ji W, He Z. Molecular mapping of quantitative trait loci for kernel morphology traits in a non-1BL.1RS1BL.1RS wheat cross. Crop and Pasture Science. 2011; 62(8): 625–638. https://doi.org/10.1071/CP11037.
49. Griffiths S, Wingen L, Pietragalla J, Garcia G, Hasan A, Miralles D, Calderini DF, Ankleshwaria JB, Waite ML, Simmonds J, Snape J, Reynolds M. Genetic dissection of grain size and grain number trade-offs in CIMMYT wheat germplasm. PLoS ONE. 2015; 10(3): 1–18. https://doi.org/10.1371/journal.pone.0118847.
50. Zhang X, Larson SR, Gao L, Teh SL, DeHaan LR, Fraser M, Sallam A, Kantarski T, Frels K, Poland J, Wyse D, Anderson JA. Uncovering the Genetic Architecture of Seed Weight and Size in Intermediate Wheatgrass through Linkage and Association Mapping. The Plant Genome. 2017; 10(3): 1–15. https://doi.org/10.3835/plantgenome2017.03.0022.
51. Cui F, Ding A, Li J, Zhao C, Li X, Feng D, Wang X, Wang L, Gao J, Wang H. Wheat kernel dimensions: How do they contribute to kernel weight at an individual QTL level? Journal of Genetics. 2011: 90(3): 409–425. https://doi.org/10.1007/s12041-011-0103-9.
52. Ramya P, Chaubal A, Kulkarni K, Gupta L, Kadoo N, Dhaliwal HS, Chhuneja P, Lagu M, Gupta V. QTL mapping of 1000-kernel weight, kernel length, and kernel width in bread wheat (*Triticum aestivum* L.). Journal of Applied Genetics. 2010; 51(4): 421–429. https://doi.org/10.1007/BF03208872.
53. Hasan AK, Herrera J, Lizana C, Calderini DF. Carpel weight, grain length and stabilized grain water content are physiological drivers of grain weight determination of wheat. Field Crops Research. 2011;

123(3): 241–247. https://doi.org/10.1016/j.fcr.2011.05.019.

54. Ma Y, Chen G, Zhang L, Liu Y, Liu D, Wang J, Pu Z, Zhang L, Lan X, Wei Y, Liu C, Zheng Y. QTL Mapping for Important Agronomic Traits in Synthetic Hexaploid Wheat Derived from Aegiliops tauschii ssp. tauschii. Journal of Integrative Agriculture. 2014; 13: 1835–1844. https://doi.org/10.1016/S2095-3119(13)60655-3.
55. Li M, Wang Z, Liang Z, Shen W, Sun F, Xi Y, Liu S. Quantitative trait loci analysis for kernel-related characteristics in common wheat (*Triticum aestivum* L.). Crop Science. 2015; 55(4): 1485–1493. https://doi.org/10.2135/cropsci2014.09.0616.
56. Qu X, Liu J, Xie X, Xu Q, Tang H, Mu Y, Pu Z, Li Y, Ma J, Gao Y, Jiang Q, Liu Y, Chen G, Wang J, Qi P, Habib A, Wei Y, Zheng Y, Lan X, Ma J. Genetic Mapping and Validation of Loci for Kernel-Related Traits in Wheat (*Triticum aestivum* L.). Frontiers in Plant Science. 2021; 12: 1–17. https://doi.org/10.3389/fpls.2021.667493.
57. Schierenbeck M, Alqudah AM, Lohwasser U, Tarawneh RA, Simón MR, Börner A. Genetic dissection of grain architecture-related traits in a winter wheat population. BMC Plant Biol. 2021; 21: 417-431. https://doi.org/10.1186/s12870-021-03183-3.
58. Cui F, Zhao C, Ding A, Li J, Wang L, Li X, Bao Y, Li J, Wang H. Construction of an integrative linkage map and QTL mapping of grain yield-related traits using three related wheat RIL populations. Theoretical and Applied Genetics. 2014; 127(3): 659–675. https://doi.org/10.1007/s00122-013-2249-8.
59. Wu QH, Chen YX, Zhou SH, Fu L, Chen JJ, Xiao Y, Zhang D, Ouyang SH, Zhao XJ, Cui Y, Zhang DY, Liang Y, Wang ZZ, Xie JZ, Qin JX, Wang GX, Li DL, Huang YL, Yu MH, Liu ZY. High-density genetic linkage map construction and QTL mapping of grain shape and size in the wheat population Yanda1817 x Beinong6. PLoS ONE. 2015; 10(2): 1–17. https://doi.org/10.1371/journal.pone.0118144.
60. Lizana XC, Riegel R, Gomez LD, Herrera J, Isla A, McQueen-Mason SJ, Calderini, DF. Expansins expression is associated with grain size dynamics in wheat (*Triticum aestivum* L.). Journal of Experimental Botany. 2010; 61(4): 1147–1157. https://doi.org/10.1093/jxb/erp380.
61. Xie Q, Mayes S, Sparkes DL. Carpel size, grain filling, and morphology determine individual grain weight in wheat. Journal of Experimental Botany. 2015; 66(21): 6715–6730. https://doi.org/10.1093/jxb/erv378.
62. Breseghello F, Sorrells ME. QTL analysis of kernel size and shape in two hexaploid wheat mapping populations. Field Crops Research. 2007; 101(2): 172–179. https://doi.org/10.1016/j.fcr.2006.11.008.
63. Williams K, Munkvold J, Sorrells M. Comparison of digital image analysis using elliptic Fourier descriptors and major dimensions to phenotype seed shape in hexaploid wheat (*Triticum aestivum* L.). Euphytica. 2013; 190(1): 99–116. https://doi.org/10.1007/s10681-012-0783-0.
64. Okamoto Y, Nguyen AT, Yoshioka M, Iehisa M, Takumi S. Identification of quantitative trait loci controlling grain size and shape in the D genome of synthetic hexaploid wheat lines. Breeding

Science. 2013; 63(4): 423–429. https://doi.org/10.1270/jsbbs.63.423.

65. Huang Y, Kong Z, Wu X, Cheng R, Yu D, Ma Z. Characterization of three wheat grain weight QTLs that differentially affect kernel dimensions. Theoretical and Applied Genetics. 2015; 128(12): 2437–2445. https://doi.org/10.1007/s00122-015-2598-6.
66. Bhusal N, Sarial AK, Sharma P, Sareen S. Mapping QTLs for grain yield components in wheat under heat stress. PLoS ONE. 2017; 12(12): e0189594. https://doi.org/10.1371/journal.pone.0189594.
67. Desiderio F, Zarei L, Licciardello S, Cheghamirza K, Farshadfar E, Virzi N, Sciacca F, Bagnaresi P, Battaglia R, Guerra D, Palumbo M, Cattivelli L, Mazzucotelli E. Genomic regions from an iranian landrace increase kernel size in durum wheat. Frontiers in Plant Science. 2019; 10: 1–21. https://doi.org/10.3389/fpls.2019.00448.
68. Xin F, Zhu T, Wei S, Han Y, Zhao Y, Zhang D, Ma L, Ding Q. QTL Mapping of Kernel Traits and Validation of a Major QTL for Kernel Length-Width Ratio Using SNP and Bulked Segregant Analysis in Wheat. Scientific Reports. 2020; 10(25): 1–12. https://doi.org/10.1038/s41598-019-56979-7.
69. Li M, Yang R, Li Y, Cui G, Wang Z, Xi Y, Liu S. QTL analysis of kernel characteristics using a recombinant inbred lines (RILs) population derived from the cross of *Triticum polonicum* L. and *Triticum aestivum* L. line "Zhong 13". Journal of Triticeae Crops. 2012; 32: 813–819.
70. Mir RR, Kumar N, Jaiswal V, Girdharwal N, Prasad M, Balyan HS, Gupta PK. Genetic dissection of grain weight in bread wheat through quantitative trait locus interval and association mapping. Molecular Breeding. 2012; 29(4): 963–972. https://doi.org/10.1007/s11032-011-9693-4.
71. Saini DK, Chopra Y, Pal N, Chahal A, Srivastava P, Gupta PK. Meta-QTLs, ortho-MQTLs and candidate genes for nitrogen use efficiency and root system architecture in bread wheat (*Triticum aestivum* L.). Physiology and Molecular Biology of Plants. 2021; 27: 2245–2267. https://doi.org/10.1007/s12298-021-01085-0.
72. Quraishi UM, Pont C, Ain QU, Flores R, Burlot L, Alaux M, Quesneville H, Salse J. Combined genomic and genetic data integration of major agronomical traits in bread wheat (*Triticum aestivum* L.). Frontiers in Plant Science. 2017; 8: 1843-1852. https://doi.org/10.3389/fpls.2017.01843.
73. Soriano JM, Alvaro F. Discovering consensus genomic regions in wheat for root-related traits by QTL meta-analysis. Scientific Reports. 2019; 9(1): 10537–10551. https://doi.org/10.1038/s41598-019-47038-2.
74. Nadolska-Orczyk A, Rajchel IK, Orczyk W, Gasparis S. Major genes determining yield-related traits in wheat and barley. Theoretical and Applied Genetics. 2017; 130(6): 1081–1098. https://doi.org/10.1007/s00122-017-2880-x.
75. Sajjad M, Ma X, Habibullah Khan S, Shoaib M, Song Y, Yang W, Zhang A, Liu D. *TaFlo2-A1*, an ortholog of rice *Flo2*, is associated with thousand grain weight in bread wheat (*Triticum aestivum* L.). BMC Plant Biology. 2017; 17(164): 1–11. https://doi.org/10.1186/s12870-017-1114-3.
76. Zhang L, Zhao YL, Gao LF, Zhao GY, Zhou RH, Zhang BS, Jia JZ. (2012). *TaCKX6-D1*, the ortholog of rice *OsCKX2*, is associated with grain weight in hexaploid wheat. New Phytologist. 2012; 195(3): 574–584. https://doi.org/10.1111/j.1469-8137.2012.04194.x.

77. Hanif M, Gao F, Liu J, Wen W, Zhang Y, Rasheed A, Xia X, He Z, Cao S. *TaTGW6-A1*, an ortholog of rice *TGW6*, is associated with grain weight and yield in bread wheat. Molecular Breeding. 2016; 36(1): 1–8. https://doi.org/10.1007/s11032-015-0425-z.

78. Ma M, Wang Q, Li Z, Cheng H, Li Z, Liu X, Song W, Appels R, Zhao H. Expression of *TaCYP78A3*, a gene encoding cytochrome P450 CYP78A3 protein in wheat (*Triticum aestivum* L.), affects seed size. Plant Journal. 2015; 83(2): 312–325. https://doi.org/10.1111/tpj.12896.

79. Guo L, Ma M, Wu L, Zhou M, Li M, Wu B, Li L, Liu X, Jing R, Chen W, Zhao H. Modified expression of *TaCYP78A5* enhances grain weight with yield potential by accumulating auxin in wheat (*Triticum aestivum* L.). Plant Biotechnology Journal. 2021; 20(1): 168-182. https://doi.org/10.1111/pbi.13704

80. Zhang K, Wang J, Zhang L, Rong C, Zhao F, Peng T, Li H, Cheng D, Liu X, Qin H, Zhang A, Tong Y, Wang D. Association Analysis of Genomic Loci Important for Grain Weight Control in Elite Common Wheat Varieties Cultivated with Variable Water and Fertiliser Supply. PLoS ONE. 2013; 8(3): e57853. https://doi.org/10.1371/journal.pone.0057853.

81. Jones BH, Blake NK, Heo HY, Martin JM, Torrion JA, Talbert LE. Allelic response of yield component traits to resource availability in spring wheat. Theoretical and Applied Genetics. 2020; 134(2): 603-620. https://doi.org/10.1007/s00122-020-03717-7.

82. E Z, Zhang Y, Li T, Wang L, Zhao H. Characterization of the ubiquitin-conjugating enzyme gene family in rice and evaluation of expression profiles under abiotic stresses and hormone treatments. PLoS ONE. 2015; 10(4): e0122621. https://doi.org/10.1371/journal.pone.0122621.

83. Mathan J, Singh A, Ranjan A. Sucrose transport in response to drought and salt stress involves ABA-mediated induction of *OsSWEET13* and *OsSWEET15* in rice. Physiologia Plantarum. 2021; 171(4): 620–637. https://doi.org/10.1111/ppl.13210.

84. Gao Y, Wang ZY, Kumar V, Xu XF, Yuan DP, Zhu XF, Li TY, Jia B, Xuan YH. Genome-wide identification of the *SWEET* gene family in wheat. Gene. 2018; 642: 284–292. https://doi.org/10.1016/j.gene.2017.11.044.

85. Gautam T, Saripalli G, Gahlaut V, Kumar A, Sharma PK, Balyan HS, Gupta PK. Further studies on sugar transporter (*SWEET*) genes in wheat (*Triticum aestivum* L.). Molecular Biology Reports. 2019; 46: 2327–2353. https://doi.org/10.1007/s11033-019-04691-0.

86. Mizuta Y, Harushima Y, Kurata N. Rice pollen hybrid incompatibility caused by reciprocal gene loss of duplicated genes. Proceedings of the National Academy of Sciences of the United States of America. 2010; 107(47): 20417–20422. https://doi.org/10.1073/pnas.1003124107.

87. Abe Y, Mieda K, Ando T, Kono I, Yano M, Kitano H, Iwasaki Y. The SMALL AND ROUND SEED1 (*SRS1/DEP2*) gene is involved in the regulation of seed size in rice. Genes and Genetic Systems. 2010; 85(5): 327–339. https://doi.org/10.1266/ggs.85.327.

88. Liu Y, Xia X, He Z. Characterization of Dense and Erect Panicle 1 Gene (*TaDep1*) Located on Common Wheat Group 5 Chromosomes and Development of Allele-Specific Markers. Acta Agronomica Sinica. 2013; 39(4): 589-598. https://doi.org/10.3724/sp.j.1006.2013.00589.

89. Xu H, Zhang R, Wang M, Li L, Yan L, Wang Z, Zhu J, Chen X, Zhao A, Su Z, Xing J, Sun Q, Ni Z. Identification and characterization of QTL for spike morphological traits, plant height and heading date derived from the D genome of natural and resynthetic allohexaploid wheat. Theoretical and Applied Genetics. 2021; 135: 389-403. https://doi.org/10.1007/s00122-021-03971-3.
90. Aoi Y, Hira H, Hayakawa Y, Liu H, Fukui K, Dai X, Tanaka K, Hayashi K, Zhao Y, Kasahara H. UDP-glucosyltransferase UGT84B1 regulates the levels of indole-3-acetic acid and phenylacetic acid in Arabidopsis. Biochemical and Biophysical Research Communications. 2020; 532(2): 244–250. https://doi.org/10.1016/j.bbrc.2020.08.026.
91. Yang D, Li M, Liu Y, Chang L, Cheng H, Chen J, Chai S. Identification of quantitative trait loci and water environmental interactions for developmental behaviors of leaf greenness in wheat. Frontiers in Plant Science. 2016); 7: 1–16. https://doi.org/10.3389/fpls.2016.00273.
92. Li M, Liu Y, Ma J, Zhang P, Wang C, Su J, Yang D. Genetic dissection of stem WSC accumulation and remobilization in wheat (*Triticum aestivum* L.) under terminal drought stress. BMC Genetics. 2020; 21(50): 1–14. https://doi.org/10.1186/s12863-020-00855-1.
93. Yang D, Liu Y, Cheng H, Chang L, Chen J, Chai S, Li M. Genetic dissection of flag leaf morphology in wheat (*Triticum aestivum* L.) under diverse water regimes. BMC Genetics. 2016; 17(94); 1–15. https://doi.org/10.1186/s12863-016-0399-9.
94. Zadoks JC, Chang TT, Konzak CF. A decimal code for the growth stages of cereals. Weed Research. 1974; 14(6): 415–421. https://doi.org/10.1111/j.1365-3180.1974.tb01084.x.
95. Toker C. Estimates of broad-sense heritability for seed yield and yield criteria in faba bean (*Vicia faba* L.). Hereditas. 2004; 140(3): 222–225. https://doi.org/10.1111/j.1601-5223.2004.01780.x.
96. Yang D, Zhang G, Li X, Xin H, Chen H, Ni S, Chen X. Genetic characteristics associated with drought tolerance of plant height and thousand-grain mass of recombinant inbred lines of wheat. Chinese Journal of Applied Ecology. 2012; 23: 1569–1576.
97. Meng L, Li H, Zhang L, Wang J. QTL IciMapping: Integrated software for genetic linkage map construction and quantitative trait locus mapping in biparental populations. Crop Journal. 2015); 3(3): 269–283. https://doi.org/10.1016/j.cj.2015.01.001.
98. Hackett CA. Statistical methods for QTL mapping in cereals. Plant Molecular Biology. 2002; 48(5): 585–599. https://doi.org/10.1023/A:1014896712447.
99. Yu K, Liu D, Chen Y, Wang D, Yang W, Yang W, Yin L, Zhang C, Zhao S, Sun J, Liu C, Zhang A. Unraveling the genetic architecture of grain size in einkorn wheat through linkage and homology mapping and transcriptomic profiling. Journal of Experimental Botany. 2019; 70(8): 4671–4687. https://doi.org/10.1093/jxb/erz247.
100. Sosnowski O, Charcosset A, Joets J. Biomercator V3: An upgrade of genetic map compilation and quantitative trait loci meta-analysis algorithms. Bioinformatics. 2012; 28(15): 2082–2083. https://doi.org/10.1093/bioinformatics/bts313.
101. Darvasi A, Soller M. A simple method to calculate resolving power and confidence interval of QTL map location. Behavior Genetics. 1997; 27(2): 125–132. https://doi.org/10.1023/A:1025685324830.

102. Veyrieras JB, Goffinet B, Charcosset A. MetaQTL: A package of new computational methods for the meta-analysis of QTL mapping experiments. BMC Bioinformatics. 2007; 8(1): 49. https://doi.org/10.1186/1471-2105-8-49.

103. Arcade A, Labourdette A, Falque M, Mangin B, Chardon F, Charcosset A, Joets J. BioMercator: Integrating genetic maps and QTL towards discovery of candidate genes. Bioinformatics. 2004; 20(14): 2324–2326. https://doi.org/10.1093/bioinformatics/bth230.

104. Borrill P, Ramirez-Gonzalez R, Uauy C. expVIP: A customizable RNA-seq data analysis and visualization platform. Plant Physiology. 2016; 170(4): 2172–2186. https://doi.org/10.1104/pp.15.01667.

105. Ramírez-González RH, Borrill P, Lang D, Harrington SA, Brinton J, Venturini L, Davey M, Jacobs J, Van Ex F, Pasha A, Khedikar Y, Robinson SJ, Cory AT, Florio T, Concia L, Juery C, Schoonbeek H, Steuernagel B, Xiang D, Uauy C. The transcriptional landscape of polyploid wheat. Science. 2018; 361(6403): 662. https://doi.org/10.1126/science.aar6089.

Figures

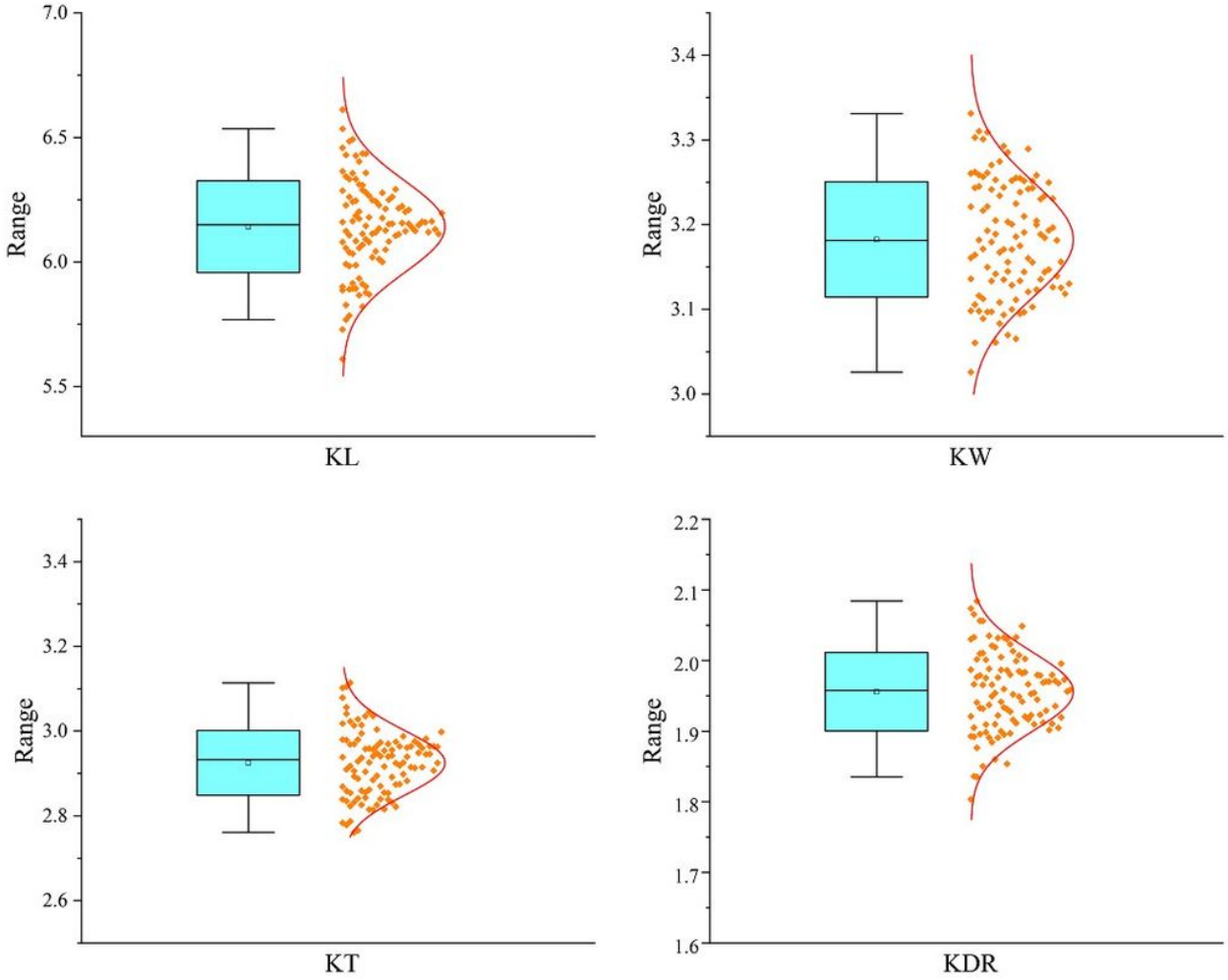

Figure 1

The frequency distribution of kernel size-related traits.

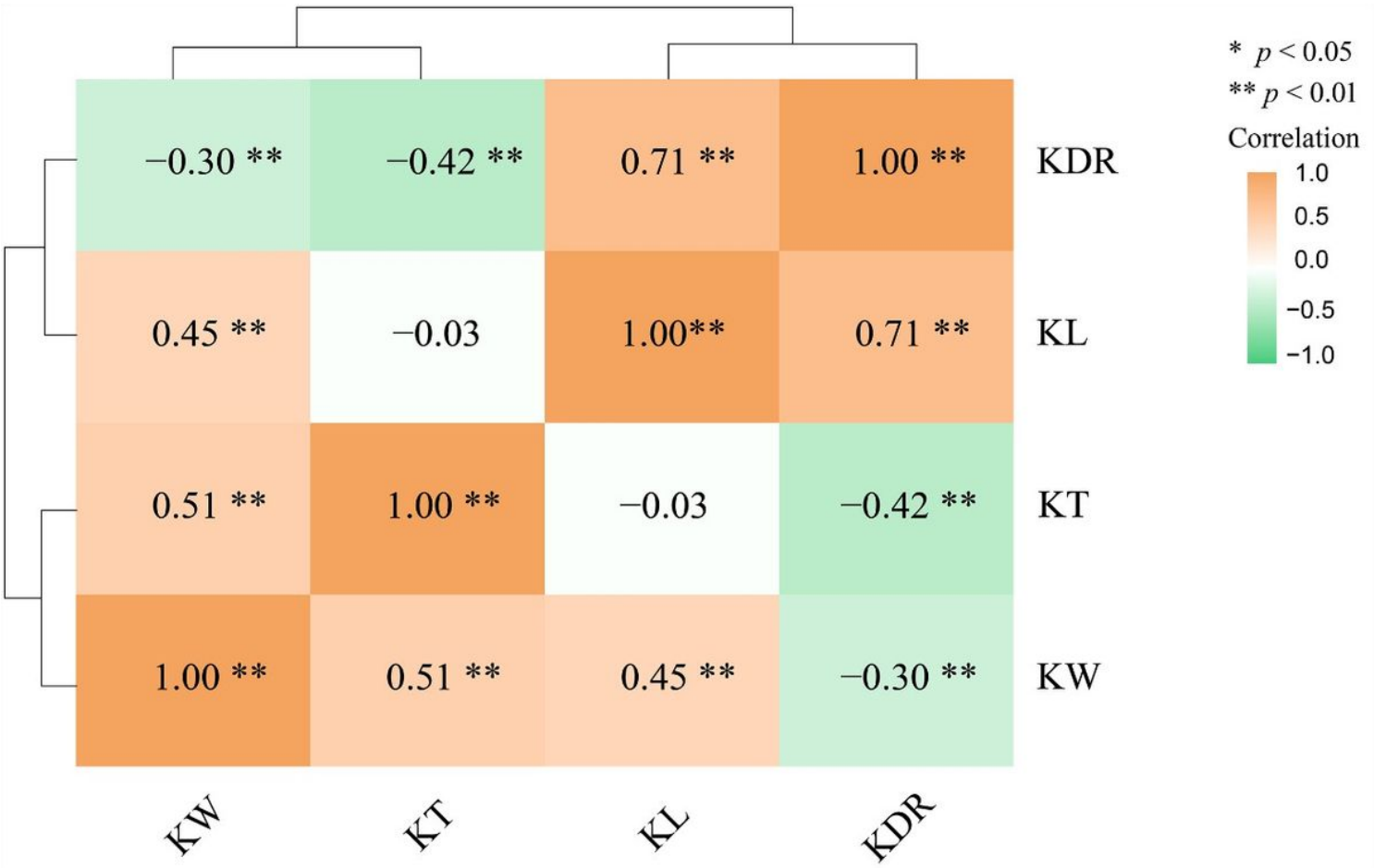

Figure 2

Correlation coefficient among four kernel size-related traits in the Q9086/Longjian19 RILs population. * and ** indicate significant level at $P < 0.05$ and $P < 0.01$, respectively.

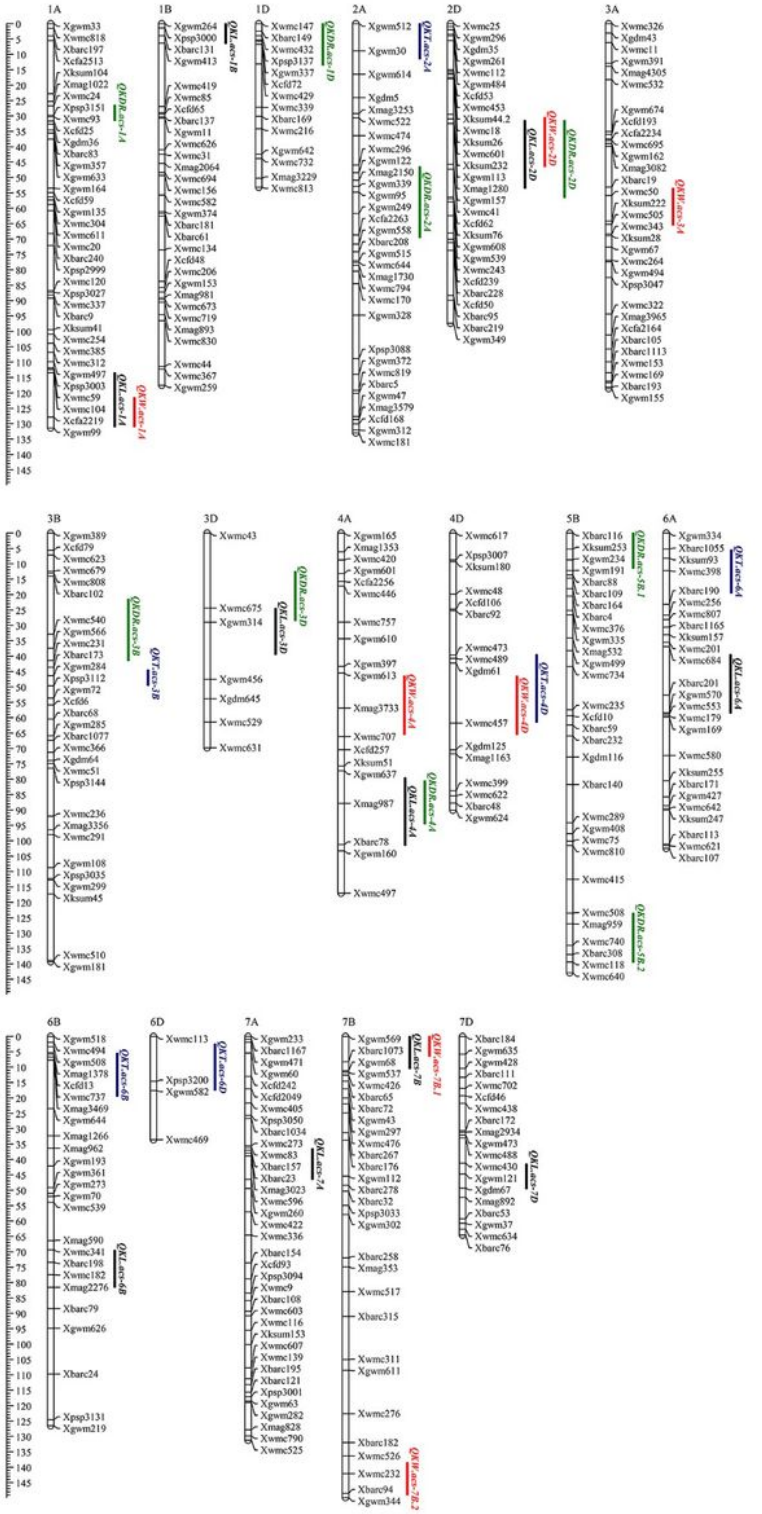

Figure 3

Chromosomal locations of QTLs detected for kernel size-related traits. The vertical bars with different colors represent interval of QTLs for kernel length (black), kernel width (red), kernel diameter ratio (green), and kernel thickness (blue).

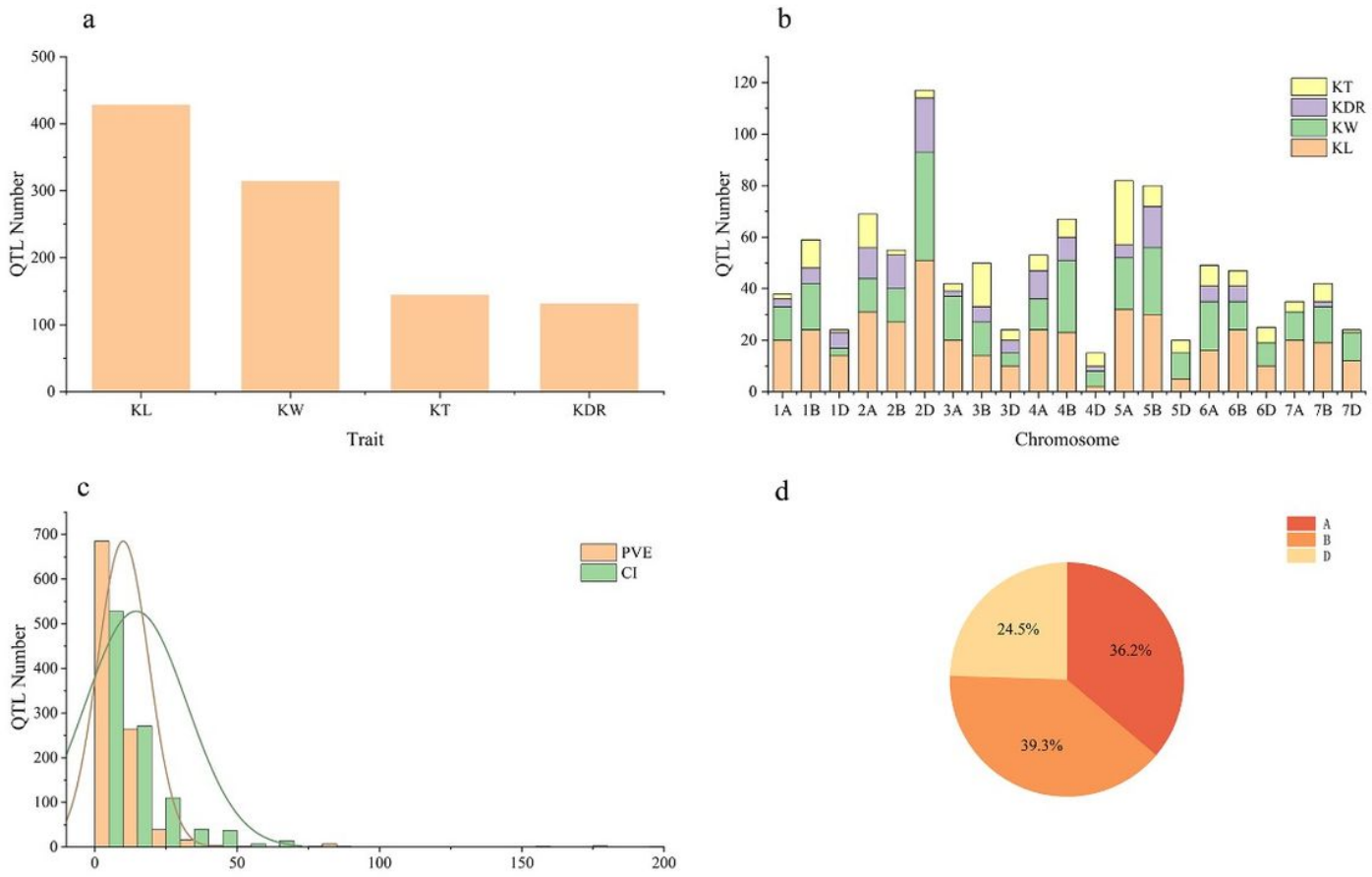

Figure 4

Number of QTLs collected (a) by trait category, KL (kernel length), KW (kernel width), KT (kernel thickness), and KDR (kernel diameter ratio) and (b) in 21 wheat chromosomes (c) frequencies of QTLs with different PVE (%) and CI values and (d) proportion of QTL numbers in wheat sub-genomes A, B, and D.

Figure 5

The chromosome distribution of the 58 MQTL for kernel size-related traits on 11 chromosomes. The circles from inside to outside represent high-density consensus genetic map, number of initial QTL which mapped on MQTL interval, values of confidence interval, values of phenotypic variation explained, and physical map, respectively.

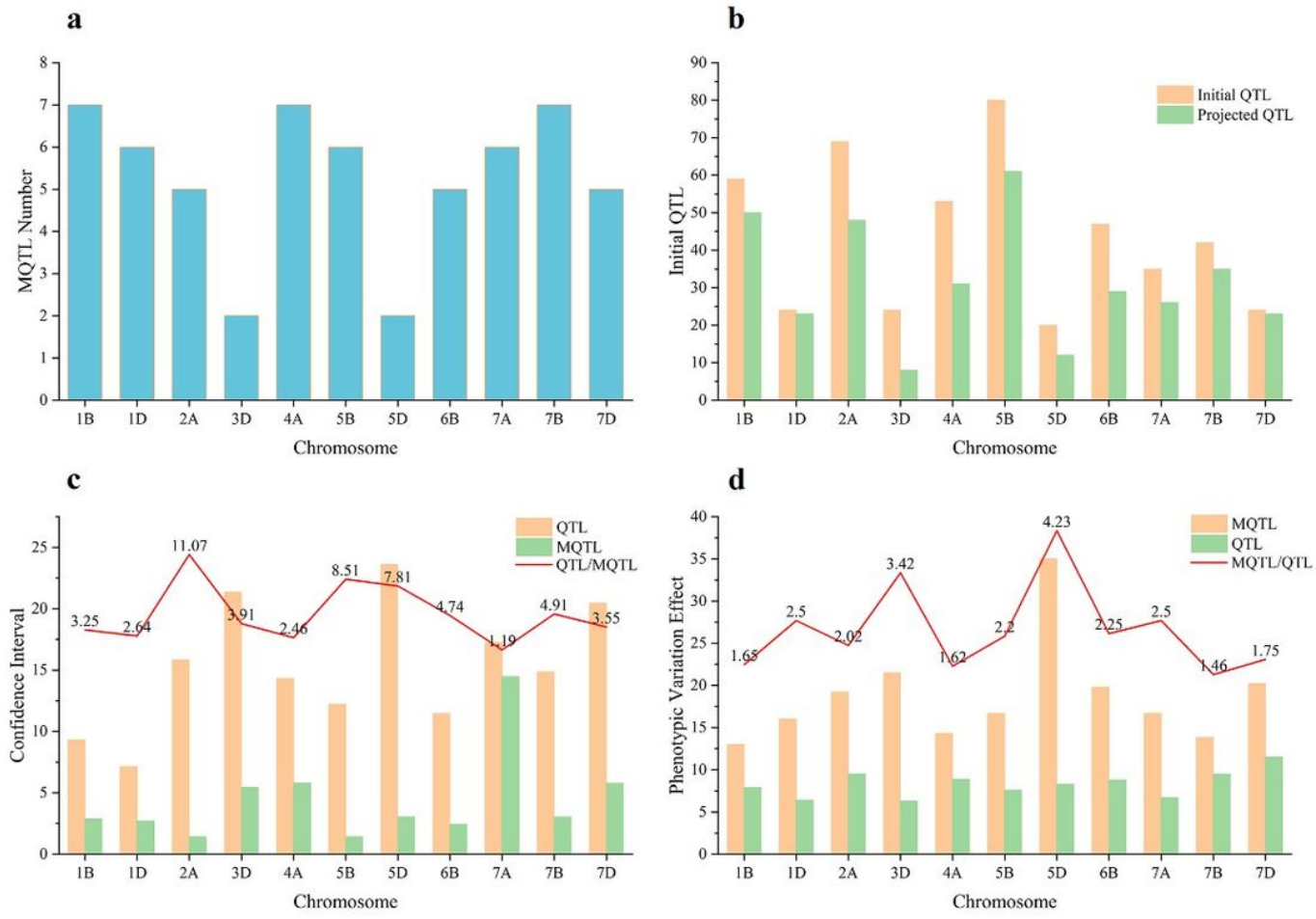

Figure 6

Number of MQTLs on different wheat chromosomes **(a)**; comparison of the original QTLs and the projected QTLs located in the MQTL intervals on different chromosomes **(b)**; comparison between the mean CI of the original QTLs and the MQTLs **(c)**; comparison between the mean PVE of the MQTLs and the original QTLs **(d)**. The numbers above the bars show the rate of change for the mean CI and PVE between the MQTLs and the original QTLs in **(c)** and **(d)**, respectively.

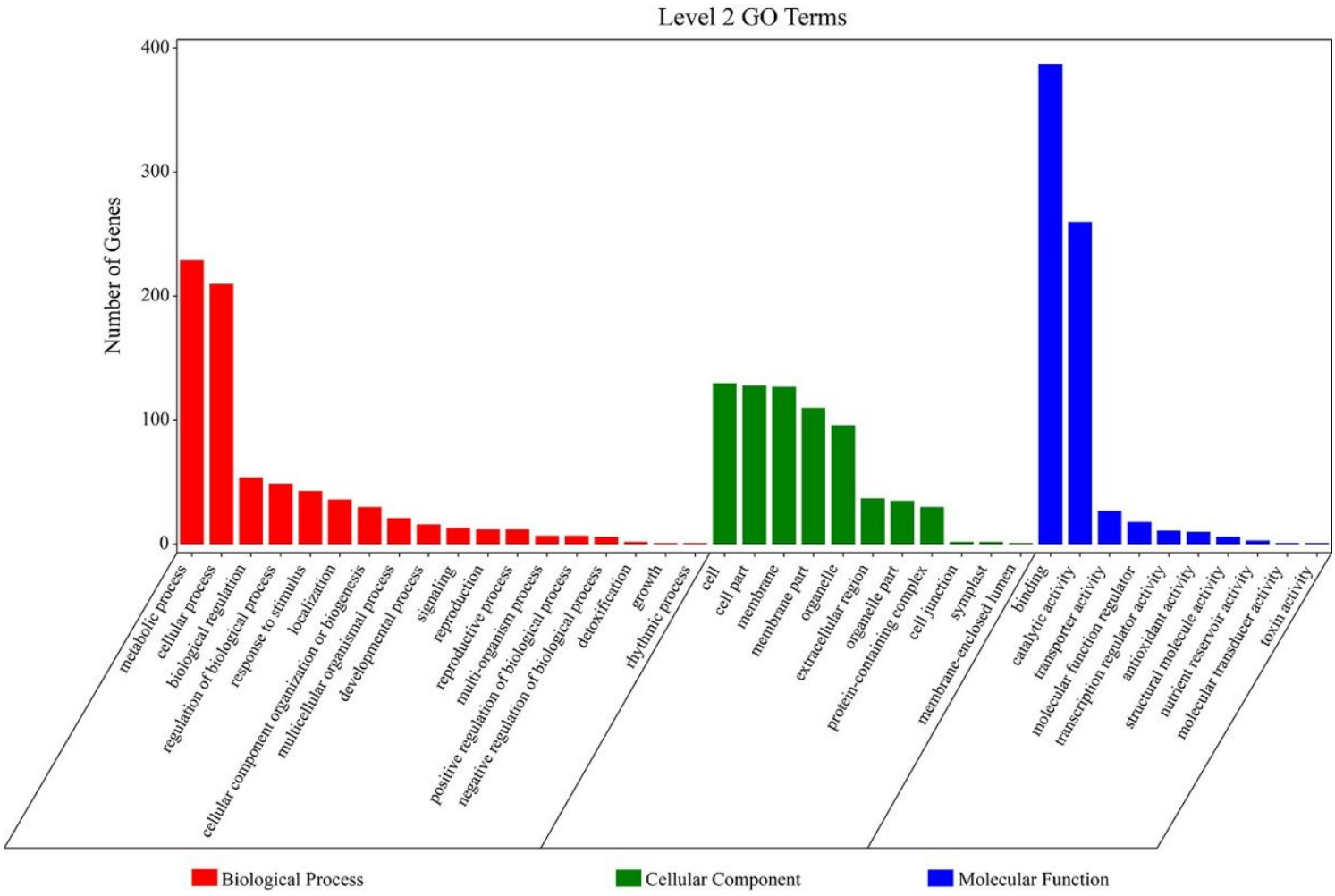

Figure 7

Gene ontology (GO) terms for 1863 candidate genes underlying MQTLs interval for kernel size-related traits.

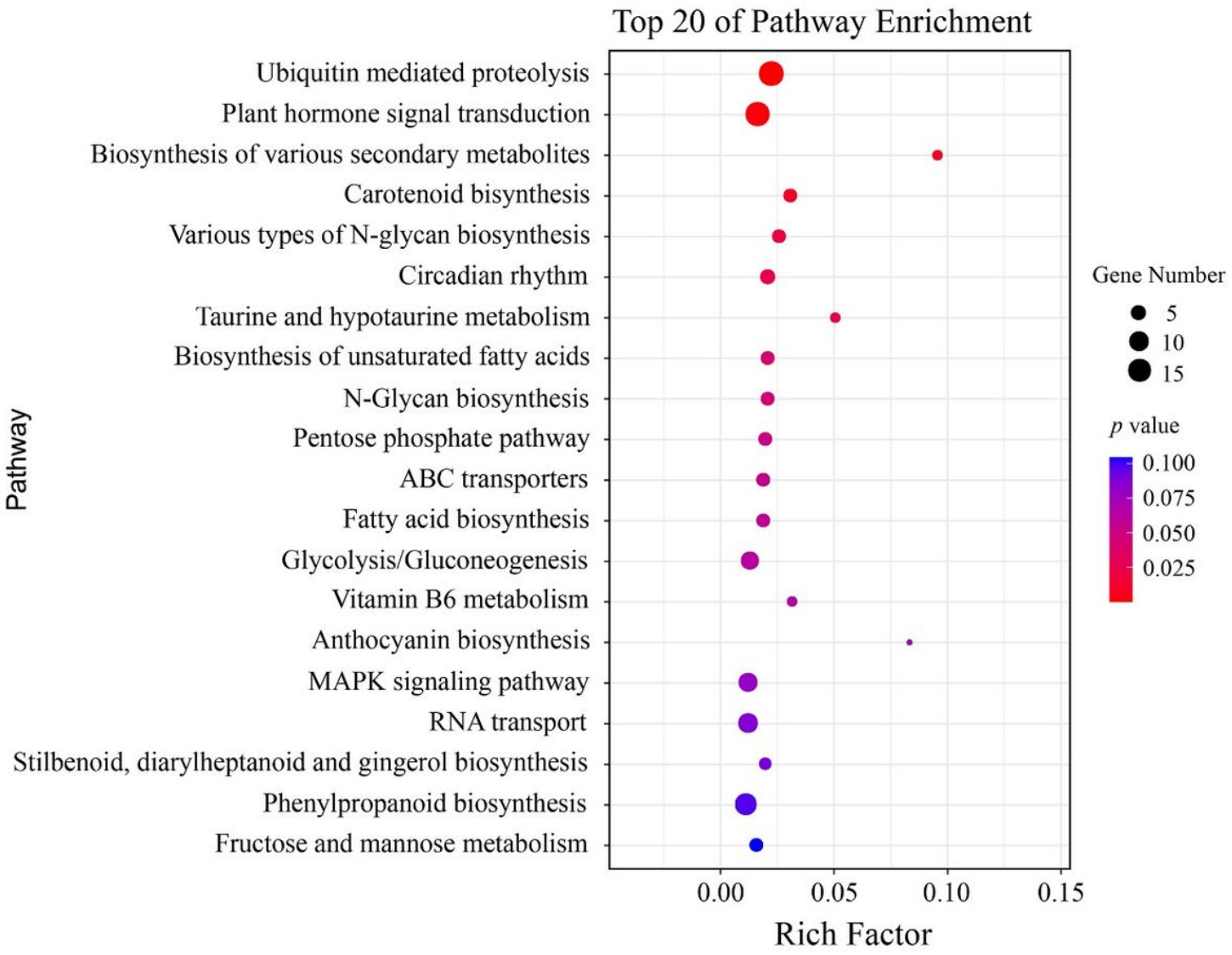

Figure 8

KEGG pathway enrichment of 1863 candidate genes.

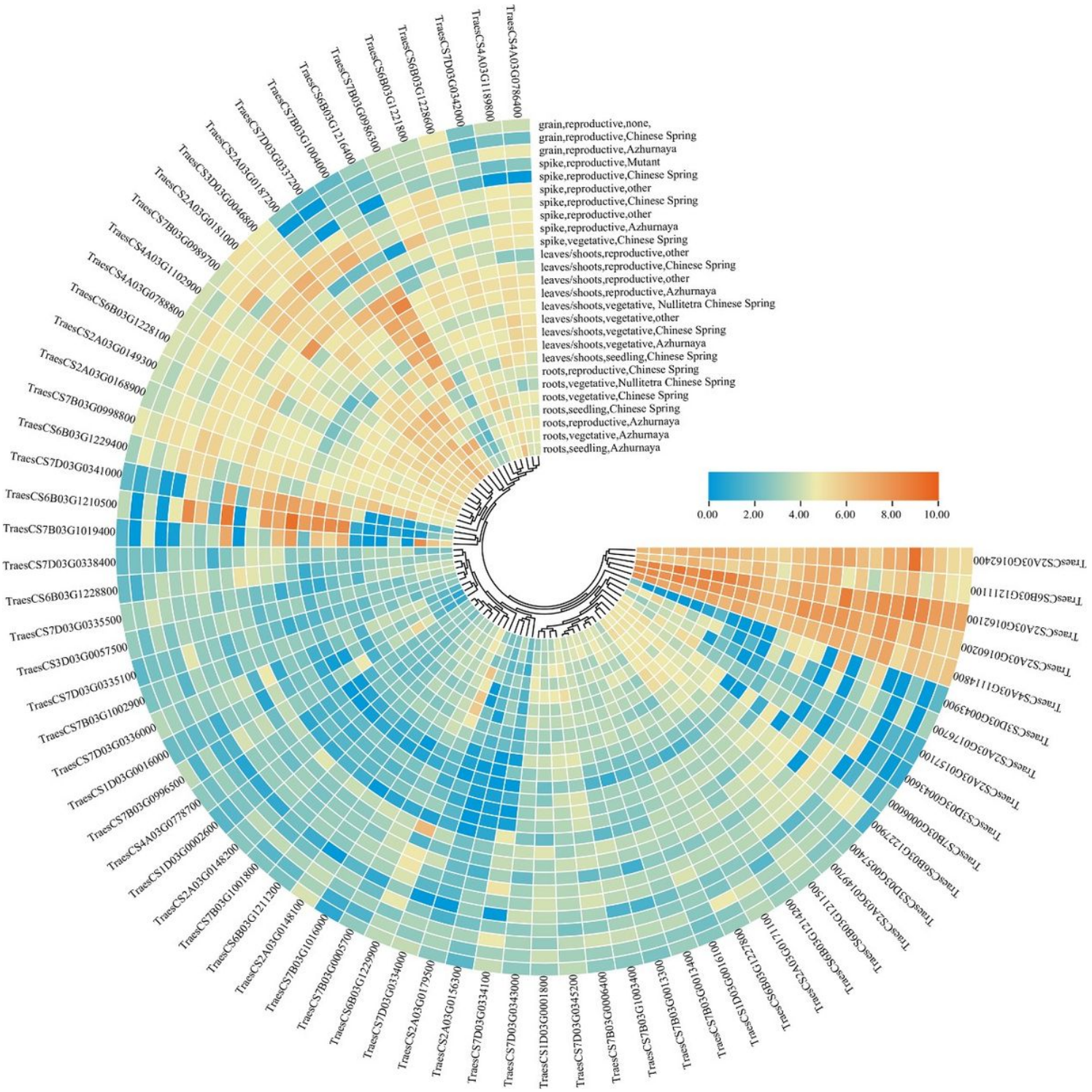

Figure 9

Heatmap showing differential expression level of 70 candidate genes underlying MQTL intervals.

Supplementary Files

This is a list of supplementary files associated with this preprint. Click to download.

- AdditionalFile1.docx
- AdditionalFile2.xlsx